Femtosecond ionization mass spectrometry for chromatographic detection

Imasaka, Totaro
Kyushu University

Imasaka, Tomoko
Department of Environmental Design, Faculty of Design, Kyushu University

出版情報：Journal of Chromatography A. 1642, pp.462023-, 2021-04-12. Elsevier
バージョン：
権利関係：

Femtosecond ionization mass spectrometry for chromatographic detection

Totaro Imasaka [a,b], Tomoko Imasaka[c,*]

[a] *Kyushu University, 744 Motooka, Nishi-ku, Fukuoka 819-0395, Japan*

[b] *Hikari Giken, Co., 2-10-30, Sakurazaka, Chuou-ku, Fukuoka 810-0024, Japan*

[c] *Department of Environmental Design, Faculty of Design, Kyushu University, 4-9-1, Shiobaru, Minami-ku, Fukuoka 815-8540, Japan*

* Corresponding author.

E-mail address: imasaka@design.kyushu-u.ac.jp (Tomoko Imasaka).

ABSTRACT

Mass spectrometry is now in widespread use for the detection of the analytes separated by chromatography. Electron ionization is the most frequently used method in mass spectrometry. However, this ionization technique sometimes suffers from extensive fragmentation of analytes, which makes identification difficult. A photoionization technique has been developed for suppressing this fragmentation and for subsequently observing a molecular ion. A variety of lasers have been employed for the sensitive and selective ionization of organic compounds. A femtosecond laser has a high peak power and is preferential for efficient ionization as well as for suppressing fragmentation, providing valuable information concerning molecular weight and chemical structure as well. In this review, we report on applications of femtosecond ionization mass spectrometry combined with gas chromatography.

Keywords: Femtosecond laser, Multiphoton ionization, Mass spectrometry, Molecular ion, Gas chromatography.

1. Introduction

Chromatography is essential for analyzing numerous constituents in real samples, since they need to be separated before spectrometric analysis. Mass spectrometry (MS) is now widely used for the detection of organic compounds, because of its excellent performance in terms of sensitivity and selectivity. Figure 1 shows a schematic example of a mass spectrum. When a molecular ion is observed, the molecular weight of the analyte can be readily determined. When the intensity distribution of the isotopomers can be measured, the number of elements such as carbon and chlorine can be determined from the natural abundance of the isotopes (^{12}C:^{13}C = 100:1 and ^{35}Cl:^{37}Cl = 3:1). As a result, a chemical formula can be obtained and used for the assignment of the analyte. Fragment ions provide information concerning the functional groups in a molecule, which is useful for determining the structure of the molecule. It should be noted that the number of mass spectra reported to date exceeds 1,000,000 and the analyte can be assigned immediately when the mass spectrum is available in the database.

Among many ionization techniques in MS, electron ionization (EI) is most frequently used, because of its simplicity and low cost for manufacturing such device. However, it is sometimes difficult to observe a molecular ion, since the energy of the electrons used for elastic collision is typically adjusted to 70 eV and is sufficient for decomposing a molecule. A variety of techniques have been developed to solve this problem. For example, while chemical ionization is a traditionally used technique, it provides a few adduct ions, which makes the structural determination of a molecular ion difficult. Electrospray ionization is useful for observing a molecular ion especially for macromolecules and can be combined with a separation technique such as liquid chromatography [1]. However, many multiply-charged molecular ions are simultaneously observed, making identification and structural analysis difficult. Matrix-assisted laser desorption ionization is a well-known technique for observing a singly-charged molecular ion [2]. However, it is difficult to combine this with a separation technique such as chromatography.

Photoionization has been developed as a technique for soft ionization, since the ionization energy can be controlled by changing the wavelength of the light source [3,4]. In fact, a vacuum ultraviolet (VUV) emission can be used for single photon ionization of various organic compounds with different spectroscopic properties. A VUV lamp is simple and is convenient to use [5]. However, an incoherent light cannot be tightly focused onto a small ionization chamber, making the application to a chromatographic detector difficult. An optical pulse produced by the third harmonic generation (118 nm) in a rare gas (Xe) using the UV pulse generated by the third harmonic generation (355 nm) of an

intense Nd:YAG laser (1064 nm) is coherent and can be tightly focused onto a small volume for use as a chromatography detector [6]. A facility of synchrotron orbit radiation has been utilized as a light source in MS coupled with gas chromatography (GC) [7].

Multiphoton ionization (MPI), one of the categories of photoionization, has been employed in numerous studies. In this case, a small-frame ultraviolet (UV) nanosecond laser can be conveniently used for MPI in MS. As shown in Figure 2 (A), when the wavelength of a laser coincides with one of the electronic-excited states, a molecule can be efficiently ionized by absorbing the first photon for excitation and a subsequent photon for ionization, a process that is referred to as resonance-enhanced two-photon ionization (RE2PI) or more generally as resonance-enhanced MPI (REMPI). This approach has been successfully used for a selective ionization of an aromatic compound by using a narrow-band tunable laser and decreasing the band width of the spectrum by supersonic jet expansion of the molecule with an inert gas, such as argon, into a vacuum [8]. When a molecule relaxes to a triplet state by intersystem crossing or the ground state by internal conversion, the lifetime of the electronic-excited state becomes shorter than the pulse width of the laser, resulting in poor ionization efficiency [9,10]. To avoid this undesirable effect, a laser with a shorter pulse width can be used, since it allows MPI via the singlet-excited state before relaxation to the triplet state [11-13]. It is possible to use a near-infrared (NIR) laser for MPI. Due to the small energy of the NIR photon, more than 10 photons are required for ionization, but this approach is rather efficient because a large pulse energy is available for a NIR laser. When a molecular ion has an absorption band at the wavelength of the NIR laser, the NIR photon is efficiently absorbed by the molecular ion, with the generation of fragment ions [14].

Many organic compounds can be measured by MS. For example, an aliphatic hydrocarbon with no π electrons has been measured in various samples, whose excitation energy is much larger than half of the ionization energy, as shown in Figure 2 (B). Since no intermediate level can be used, the molecule should be ionized through a nonresonant process, which is referred to as nonresonant two-photon ionization (NR2PI) or more generally as nonresonant MPI (NRMPI). Ionization efficiency can be increased by increasing the laser pulse energy and by tightly focusing the laser beam, but fragmentation is unavoidable under such conditions. It would be possible to use a laser emitting at shorter wavelength for RE2PI, but this would increase the excess energy remaining in the ionic state, which would, in turn, accelerate the extent of fragmentation. This problem can be solved by using a high-peak-power low-pulse-energy laser, which can be achieved by reducing the laser pulse width, i.e., using a UV femtosecond laser, for NR2PI [15].

A pulsed laser is useful as an ionization source in time-of-flight MS (TOFMS), allowing

comprehensive analyses to be achieved based on GC-MS. A two-dimensional GC-MS display is beneficial for the visual confirmation of numerous constituents in environmental and forensic samples. This advanced technique is verified to be useful for trace analysis of various organic compounds. However, a femtosecond laser such as a Ti:sapphire laser is expensive, large, and requires a high maintenance cost. In addition, special skill is needed for operation and maintenance. Then, the number of laboratories employing femtosecond ionization MS (FIMS) is limited at the present stage especially for application to a chromatography detector. For practical use, it would be desirable to develop a compact MS which can be combined with a high-power, low-cost, small-size, maintenance-free, and easy-to-operate femtosecond laser commercially available now. A compact TOFMS with a 6.4-cm flight tube has been developed for this purpose and has sufficient mass resolution ($m/\Delta m$ = 400) [16]. Accordingly, FIMS will become a promising tool for use as a detector for chromatography in the near future.

2. Experimental considerations

2.1. Outline

Figure 3 shows a block diagram of the experimental apparatus when GC is combined with laser ionization MS. The analyte eluting from the gas chromatograph is introduced into a TOFMS. A laser beam is focused into the ionization region, and the induced ions are accelerated toward a flight tube and are measured by a microchannel plate detector. A transient signal, i.e., a mass spectrum, is recorded by an oscilloscope or a digitizer installed in a personal computer. Two-dimensional GC-MS data can be monitored on the computer screen.

2.2. Mass spectrometer

It is difficult to increase the density of the analyte in the ionization region when a sample is introduced from a side of an electrode assembly, as shown in Figure 4 (A). In contrast, the density can be increased significantly when the sample is injected behind the repeller, as shown in Figure 4 (B) [17,18]. Due to a high potential applied to the repeller electrode, the fused-silica capillary used for sample introduction needs to be isolated by a ceramic insulator. In this proximity configuration, the density of the analyte can be increased by 50-fold [19]. As shown in Figure 4 (C), the ions are accelerated by a pair of skimmer-type extraction/ground electrodes with no mesh. The extraction grid

is used to compensate for the initial spatial distribution (Δx) of the ion that is focused by an einzel lens electrode assembly and is deflected by the potentials applied to two pairs of deflector electrodes onto a microchannel plate detector. An off-axis sample introduction technique, in which the fused-silica capillary is slightly tilted away from the axis of the flight tube, was developed to reduce the collision between the analyte and the helium carrier gas [20]. The measured mass resolution was 1,600 [21]. The efficiency of ionization can be improved by 2.5 fold by introducing the molecular beam at the angle slightly off-axis with respect to the laser beam [22].

2.3. Ionization laser

The ionization mechanism depends on the laser used in the experiment. In fact, the efficiency of ionization and the degree of fragmentation are strongly affected by the pulse width and the wavelength of the laser. The pulse width can be changed by passing a femtosecond beam through a fused-silica plate that results in the dispersion of the material [15,23]. The pulse width can be calculated using equation (1). The parameter, Δt_0, represents the pulse width of the incident beam, l is the thickness of the fused-silica plate, and GVD is the group velocity dispersion calculated using the Sellmeier equation.

$$\Delta t_1 = \Delta t_0 \sqrt{1 + 16\left(ln2 \frac{l \cdot GVD}{\Delta t_0^2}\right)^2} \qquad (1)$$

To generate a shorter optical pulse, it is necessary to expand the spectral domain, as recognized from a Fourier transformation ($\Delta t \times \Delta \nu \geq 0.441$ for a Gaussian pulse where Δt and $\Delta \nu$ are the pulse width and the spectral width, respectively). When a femtosecond laser beam is focused into a noble gas such as argon, the spectral band width can be increased by self phase modulation. As a result, the pulse width can be compressed by compensating for the dispersion. Further extension of the spectral domain can be achieved by superposition of two coherent pulses with same relative phase (see the photograph for the experimental apparatus shown in Figure 5). A 3.2-fs optical pulse can be generated in the NIR region, which is then further converted into a 1.9-fs UV pulse by the third harmonic generation [24]. The measured pulse energy was 20 nJ, which is sufficient for use in MPI-MS.

The wavelength of the femtosecond laser can be converted into the NIR or UV regions based on nonlinear optical phenomena. Figure 6 shows an example of a frequency conversion system [24]. A Ti:sapphire laser (800 nm, 35 fs) is used as a fundamental laser (pump beam) of an optical parametric amplifier (OPA) to generate a tunable emission in the NIR (e.g., 1200 nm for a signal beam and 2400

nm for an idler beam). The remaining part of the Ti:sapphire laser is passed through nonlinear optical crystals (β-barium borate) for second (400 nm), third (267 nm), and fourth (200 nm) harmonic generations, which can be used for the MPI of an organic compound. For generating a VUV optical pulse, a two-color pump beam consisting of the Ti:sapphire laser (800 nm) and the OPA (1200 nm) is focused into a hydrogen gas filled in a fused-silica capillary for molecular phase modulation, which is used for frequency modulation of a probe beam (200 nm) introduced after the pump pulse. As shown in Figure 7, the VUV beam is generated by three-color four-wave Raman mixing (FWRM) at 185 nm in addition to 218, 240, and 267 nm in the UV region, the frequency separation of which is determined by a Raman shift frequency (4155 cm^{-1}) of molecular hydrogen. Several emission lines are simultaneously generated in the visible (VIS) – NIR region by two-color FWRM.

FIMS

3. Basic principles of operation

3.1. Laser parameters

Figure 8 shows a schematic of an MPI for an organic molecule. When relaxation from an intermediate state and the dissociation of a molecular ion are negligible, the signal intensity of the molecular ion can be expressed by equations (2) – (4) for RE2PI, NR2PI, and non-resonant three-photon ionization (NR3PI) processes, respectively [23]. The signal intensity is proportional to the number of molecules in the ground state, $[N_0]$, and is proportional to the square (cubic) of the pulse energy, E, in the two-photon (three-photon) process. On the other hand, the signal intensity is reciprocally proportional to the pulse width, Δt, in NR2PI and to the square of the pulse width in NR3PI. Therefore, a short optical pulse is preferred for observing a molecular ion.

$$[M^+] \propto k_1 k_2 [N_0] E^2 \quad (2)$$

$$[M^+] \propto k_{12} [N_0] E^2 \frac{1}{\Delta t} \quad (3)$$

$$[M^+] \propto k_{123} [N_0] E^3 \frac{1}{\Delta t^2} \quad (4)$$

The laser parameters that affect ionization efficiency were investigated in detail [15]. The efficiency is confirmed to be proportional to the square of the laser pulse energy and is less affected by the laser pulse width when a molecule is ionized through a RE2PI process. On the other hand, the ionization was less efficient in NR2PI (and more in NR3PI), when a molecule was ionized using a

long pulse (e.g. Δt = 700 fs). However, the signal intensity obtained by NR2PI became nearly identical to the value obtained by RE2PI at < 75 fs, suggesting that the effect of resonance by the intermediate state becomes negligible at shorter pulse widths (< 50 fs).

3.2. Excess energy

In the previous section, we assumed that a molecular ion does not undergo dissociation, in order to simplify the discussion. However, the molecular ion does, in fact, sometimes undergo dissociation, when the excess energy remaining in the ionic state is sufficiently large and can be used for dissociation. In fact, it has been reported that the wavelength of the laser can affect the efficiencies of ionization and fragmentation. When the excess energy is much larger than 1.5 eV, fragmentation becomes dominant although it depends on the molecule being examined [26]. There are two major approaches, i.e., UV and NIR ionization, as shown in Figure 2 (A). The former requires a more complicated frequency conversion system. However, a molecule can be efficiently ionized by RE2PI/NR2PI, and the three-photon process providing a large excess energy can be minimal when a UV laser with a small pulse energy is used. On the other hand, the latter requires no frequency conversion system. However, when a molecular ion has an absorption band at the wavelength of the NIR laser, it easily undergoes dissociation after absorbing an additional photon. Accordingly, the wavelength of the laser would need to be optimized to increase the ionization efficiency and to observe a molecular ion [27].

4. Chromatographic applications

4.1. Polycyclic aromatic hydrocarbons

A polycyclic aromatic hydrocarbon (PAH) with an extended π electron system absorbs a UV photon and is ionized via RE2PI. This type of compound can be efficiently ionized using a femtosecond laser as well as a nanosecond laser. In fact, subfemtogram detection limits have been reported, and this technique has been applied to the trace analysis of PAHs in surface water samples [28]. Molecular ions are observed for 16 components specified by NIST on the two-dimensional display of GC-MS.

4.2. Halogenated polycyclic aromatic hydrocarbons

As mentioned above, halogen atoms in a molecule accelerate intersystem crossing and decrease the lifetime of the excited state. Ionization from a triplet state using a deep-UV (DUV) laser shown in Figure 2 (A) can partly compensate for the decrease in ionization efficiency. However, the efficiency can be significantly improved by decreasing the laser pulse width thus achieving a more efficient RE2PI [29-31]. Figure 9 (A) shows the two-dimensional GC-MS display for a sample extracted from a soil and processed by column chromatography before the analysis. Many components arising from chlorinated biphenyl (CB), dibenzo-*p*-dioxin (CDD), dibenzofuran (CDF), naphthalene (CN), and terphenyl (CT) derivatives are observed in the two-dimensional GC-MS data. It is known that the contribution to the toxicity of such samples is determined by the concentrations of pentaCDFs because of their high toxicities and high concentrations in the environment. Figure 9 (B) shows an expanded view of the area where pentaCDFs appear [32]. Several isomers are separated by GC, and several isotopomers arising from naturally abundant ^{35}Cl and ^{37}Cl isotopes can be resolved by MS. From the intensity distribution, the number of chlorine atoms in a molecule can be confirmed to be 5, i.e., pentaCDF. Note that the isotopomers arising from naturally abundant ^{12}C and ^{13}C isotopes are also resolved by MS and the number of carbon atoms can also be confirmed to be 12. A strong signal arising from an impurity, probably due to a decomposition product of PCB, judging from the broad signal peak, is observed at a retention time of 621 s. This signal can be easily ruled out from pentaCDF on the two-dimensional GC-MS display. For quantitative analysis, ^{13}C-pentaCDF isotopomers that are artificially synthesized from the reactants comprised of only ^{13}C atoms are added to the sample for use as internal standards. Since the ionization efficiency of ^{13}C-pentaCDF is nearly identical to that of ^{12}C-pentaCDF, the concentration of the analyte can be determined from the ratio of the signal intensities for the ^{12}C- and ^{13}C-isotopomers [28,33]. Due to better background suppression performance, the process for preparing the sample can be simplified, thus decreasing the need for a lengthy pretreatment [34]. Figure 10 (A) shows data for a soil sample obtained after the Earthquake in Tohoku, Japan, suggesting that aliphatic hydrocarbons originating from petroleum are present as the major components in the soil. Figure 10 (B) shows data for a different soil sample obtained near the above location, indicating that high concentrations of PCBs are present in the sample. These data suggest that the PCB oil in a container was spread by the disaster. The PCB in a transformer oil in Vietnam was also measured using this technique [35]. PAHs substituted with bromine atoms are added to plastics for electric consumables as flame retardants. Since hazardous compounds are produced by the combustion of the plastic-containing materials, the concentration of brominated PAHs should be measured before being reused. It has been reported that the intensity of

a molecular ion can be drastically enhanced by decreasing the laser pulse width in MPIMS [36].

4.3. Nitro polycyclic aromatic hydrocarbons

It is well known that nitro polycyclic aromatic hydrocarbons (NPAHs) are strongly carcinogenic and are present in particulate matter 2.5 (PM2.5). Ionization energy is not changed significantly by the presence of a nitro group in a molecule, but a strong absorption band appears in the near-UV region (300-400 nm) [37]. Figure 11 shows mass spectra measured using a tunable femtosecond laser in the region from 267 to 405 nm [38]. Figure 12 shows a schematic energy diagram calculated for NPAHs by density functional theory using a Gaussian program. The molecules are ionized via RE2PI at a wavelength of around 267 nm, RE3PI at around 345 nm, and NR3PI at the above 405-450 nm. The fragmentation is suppressed at longer wavelengths, although the signal intensity decreases drastically. Figure 13 shows two-dimensional GC-MS displays for a sample extracted from a diesel soot sample measured at 200, 267, and 345 nm [39]. Because strong signals arising from impurities are observed at shorter wavelengths, it is desirable to measure the sample using a near-UV laser (e.g., 345 nm). In fact, NPAHs such as 9-nitroanthracene (9-NANT), 3-nitofluoranthene (3-NFLU), and 1-nitropyrene (1-NPYR) are observed in the two-dimensional GC-MS display. A two-dimensional GC-MS display of NPAHs was also measured at 400, 800, and 1200 nm [14]. Due to the large output power of the NIR laser and the absence of an absorption band in the NIR region, the signal intensity can be increased and the undesirable signals arising from impurities can be suppressed, thus allowing trace analysis of NPAHs in the complex matrix.

4.4. Allergens

Many allergens are contained in daily consumables. In the Cosmetics Directive published by the Scientific Committee for Consumer Safety, 26 ingredients that are typical components of fragrances are specified as allergens that should be listed on the label of a container when the concentrations are higher than 0.001% for leave-on products and 0.01% for rinse-off products. Figure 14 shows the chemical structures of these allergens. They have very different chemical and spectral properties and are useful for examining the advantages of FIMS [26]. It has been reported that it is difficult to observe a molecular ion in the case of a flexible molecule such as farnesol. However, the molecular ion (1% in EIMS) can be enhanced to 80% (isomer a) and 20% (isomer b) for farnesol in FIMS. Other flexible molecules such as hydroxycitronellal, geraniol, and citronellol seldom provide a molecular

ion (≤ 2%) in EIMS. Although they are ionized via NRMPI in FIMS, the molecular ion can be enhanced to 7-21%. Figure 15 shows two-dimensional GC-MS displays for two actual samples, and the difference can be immediately visually confirmed. The limits of detection obtained were <100 pg/μL for all 26 compounds, which were achieved by using the third-harmonic emission of the Ti:sapphire laser (267 nm, 130 μJ).

4.5. Pesticides

To examine the advantage of FIMS, it would be desirable to measure a sample containing various types of compounds that were not selected by the researcher. For example, a standard sample mixture containing 51 commercially available pesticides would be one of the candidates for this purpose, since it consists of very different types of aromatic/aliphatic compounds with/without heavy atoms such as chlorine and nitro groups and hetero-rings/long-side-chains as well, as shown in Figure 16 [40]. The detection limits were measured using FIMS at 267, 400, and 800 nm and were compared to discuss the optimal conditions for ionization [41]. It is interesting to note that pesticides eluting earlier from the DB5-ms column provide molecular ions in NIR FIMS, which is in contrast to the observation of molecular ions in UV FIMS for compounds that elute later. Thus, a larger molecule with a higher polarity, which elutes later from the GC column, would be preferentially ionized using a UV laser. The use of a shorter wavelength (e.g., 200 nm) is desirable for the more sensitive detection of pesticides with no aromatic rings [42,43]. Chiral species of (±)-α-hexachlorocychrohexanes can be separated by a chiral column of GC, and their molecular ions were enhanced by measuring at a short wavelength of 200 nm [43].

4.6. Explosives

Finding a compound that is difficult to measure a molecular ion by EIMS is a challenge, since the advantage of FIMS can be clearly demonstrated by observing the molecular ion. Alcohols, ethers, and peroxides would be the examples for this. An explosive such as triacetone triperoxide (TATP), which has been utilized in terrorist attacks, can be easily synthesized even by a person with little knowledge of chemistry. This compound has a flexible peroxide ring and dissociates readily, providing no molecular ion in EIMS. However, a molecular ion can be clearly observed by using a UV femtosecond laser in MS [44,45]. Figure 17 shows the mass spectrum of TATP measured at different wavelengths in the UV region [46]. A molecular ion can be measured only at the wavelength

of 267 nm, suggesting that the excess energy in the ionic state is minimal at this wavelength. Figure 18 (A) shows a two-dimensional display of GC-MS for a human blood sample containing TATP [47]. A deuterated compound, TATP-d18, was synthesized from deuterated acetone (CD_3-CO-CD_3) and was used as an internal standard to calibrate the retention time in GC and the signal intensity in MS. A molecular ion is observed both for TATP and TATP-d18, in addition to several fragment ions. In EIMS, the signal intensity of the fragment ion (e.g., $C_2H_3O^+$, Mw = 43) is used for selected ion monitoring (SIM) to construct a chromatogram. Figure 18 (B) shows a two-dimensional GC-MS display for a sample containing acetone that is frequently used for sampling the analytes. A component appears with a retention time close to that of TATP and provides a fragment peak with a molecular weight of 43. In the later study, this unknown compound was found to be phorone, i.e., $(CH3)_2C=CH-CO-CH=C(CH_3)_2$, which was produced from acetones by aldol condensation. Because of this, it would be necessary to carefully confirm the signal arising from TATP in a chromatogram that was measured by EIMS.

4.7. Chemical reactions

An actual sample contains numerous chemical species even after pretreatment. In fact, it is difficult to assign the compounds in most cases when no standard chemicals are available. However, compounds with redox functional groups can be determined by measuring the chemical species with and without redox chemical reactions. For example, a nitro compound can be converted into an amino compound using a reducing reagent. The chemical species with a nitro group can then be identified by comparing the two-dimensional GC-MS displays measured with and without the chemical reaction. In fact, an actual sample containing NPAHs was injected into the GC with and without hydrazine monohydrate ($H_2NNH_2 \cdot H_2O$) as a reducing reagent. From the two-dimensional GC-MS displays shown in Figure 19, some of the components disappeared/appeared as the result of the reaction, suggesting that NPAHs were converted into amino PAHs (APAHs) [48]. Thus, NPAHs, whose carcinogenicity is 10-100,000 times larger than the corresponding PAHs, can be identified without using standard chemicals. When a catalyst (Pt or Pd) was utilized to increase the reactivity, numerous compounds were produced by the decomposition of the aromatic rings. It is possible to react the analytes after GC separation in a fused-silica capillary by mixing the sample with hydrazine monohydrate [49]. In this on-line chemical reaction system, the mass spectrum of the product (APAH) is observed at the retention times of the reactant (NPAH). Thus, a molecule with a specific reactive site can be determined by comparing the data measured with and without introducing the reducing

reagent, providing a useful means for assignment of the analyte.

4.8. Derivatization

Many analytes contain polar functional groups and are thermally labile at high temperatures. Such molecules should be derivatized using a reagent that is reactive with respect to the polar functional group prior to GC-MS [50]. As shown in Figure 20, 2-(bromomethyl)naphthalene (BMN) contains a bromomethyl group that can react with an OH group and a naphthalene chromophore that can be efficiently ionized at 267 nm by RE2PI [51]. This compound is coupled with nerve agent metabolites such as ethyl methylphosphonic acid (EMPA), isopropyl methylphosphonic acid (IMPA), and pinacolyl methylphosphonic acid (PMPA) in human urine. All of these compounds combined with BMN can be separated on the two-dimensional GC-MS display, as shown in Figure 21. Sub-nanogram detection limits were reported for these metabolites, which were superior to the results (50 ng in full-scan mode and 2.5-10 ng in SIM) in EIMS and were comparable to the results (0.06 ng, measured after 1.3-3-fold concentration in SIM) for negative-ion chemical-ionization MS. Since a bromomethyl group can be combined with OH groups in various compounds, this derivatization scheme can be generally applied for thermally labile compounds before analysis using GC-MPIMS.

4.8. Application to fundamental studies

It is interesting to note that GC-FIMS can be used, not only for analytical purposes, but also for fundamental studies such as molecular spectroscopy. When the spectral properties of organic molecules are compared quantitatively, all of the compounds must be carefully purified, e.g., by distillation, before the measurement, and the experimental conditions such as the intensity of the light source must be kept constant if quantitative data are required for discussion. This is, however, not easy when many samples, e.g., more than 50 compounds, need to be studied simultaneously. Moreover, extremely toxic compounds need to be handled with extreme care by the researcher. However, measuring such compounds using GC-FIMS is relatively straightforward, since more than 50 compounds prepared at ppb levels or present as constituents in a complex matrix can be separated, measured, and compared quantitatively. For example, the spectral properties (e.g., the ionization efficiency) of naturally abundant products of dioxins (239 compounds) can be measured at different wavelengths and laser pulse widths. In fact, 856 compounds have been measured by FIMS to date. Thus, GC-FIMS would be a useful method for fundamental studies related to examining organic

compounds.

4. Conclusions

Chromatography requires an advanced spectrometric tool such as MS that is sensitive and can provide valuable information such as molecular weight and chemical structure. Although EIMS has been applied to a variety of organic compounds, this technique is based on elastic collisions of electrons and is difficult to control the excess energy in the ionic state, resulting in extensive fragmentation in many cases. On the other hand, the excess energy can be precisely controlled in MPIMS. When a femtosecond laser is used, the analyte can be efficiently ionized even in NR2PI, in which the excess energy remaining in the ionic state can be minimized to zero by adjusting the laser wavelength to the half value of the ionization energy. For this reason, fragmentation can be suppressed in FIMS, providing a molecular ion and large fragment ions as well. Therefore, this technique is useful for the assignment of even unknown chemical species that are not listed in the MS database (e.g., psychoactive substances illegally synthesized every year). Superior selectivity given by REMPI permits the use of simple pretreatment procedure before the measurement by chromatography. Accordingly, FIMS would have potential for use as a practical tool in advanced chromatography in the future.

Acknowledgements

This research was supported by a Grant-in-Aid for Scientific Research from the Japan Society for the Promotion of Science [JSPS KAKENHI Grant Numbers 20H02399] and by the Program of Progress 100 in Kyushu University, The Iwatani Naoji Foundation, and 2020 Collaboration Development Fund for a Joint Program between National Taiwan Normal University and Kyushu University. Quantum chemical calculations were mainly carried out using the computer facilities at the Research Institute for Information Technology, Kyushu University.

References

[1] J.B. Fenn, M. Mann, C.K. Meng, S.F. Wong, C.M. Whitehouse, Electrospray ionization for mass spectrometry of large biomolecules, Science 246 (1989) 64-71.

[2] M. Karas, F. Hillenkamp, Laser desorption ionization of proteins with molecular masses exceeding 10,000 daltons, Anal. Chem. 60 (1988) 2299-2301.

[3] U. Boesl, R. Zimmermann, C. Weickhardt, D. Lenoir, D.W. Schramm, A. Kettrup, E.W. Schlag, Resonance-enhanced multi-photon ionization: A species-selective ion source for analytical time-of-flight mass spectroscopy, Chemosphere 29 (1994) 1429–1440.

[4] T. Imasaka, Gas chromatography/multiphoton ionization/time-of-flight mass spectrometry using a femtosecond laser, Anal. Bioanal. Chem. 405 (2013) 6907–6912.

[5] Y. Wang, J. Jiang, L. Hua, K. Hou, Y. Xie, P. Chen, W. Liu, Q. Li, S. Wang, H. Li, High-pressure photon ionization source for TOFMS and its application for online breath analysis, Anal. Chem. 88 (2016) 9047−9055.

[6] R. Zimmermann, W. Welthagen, T. Gröger, Photo-ionisation mass spectrometry as detection method for gas chromatography: Optical selectivity and multidimensional comprehensive separations, J. Chromatogr. A 1184 (2008) 296–308.

[7] J.A. Nowak, R.J. Weberb, A.H. Goldsteinb, Quantification of isomerically summed hydrocarbon contributions to crude oil by carbon number, double bond equivalent, and aromaticity using gas chromatography with tunable vacuum ultraviolet ionization, Analyst 143 (2018) 1396-1405.

[8] T. Imasaka, D.S. Moore, T. Do-Dinh, Critical assessment, Use of supersonic jet spectrometry for complex mixture analysis, Pure Appl. Chem. 75 (2003) 975-998.

[9] S. Yamaguchi, T. Uchimura, T. Imasaka, Gas chromatography/multiphoton ionization/mass spectrometry of polychlorinated dibenzofurans using nanosecond and femtosecond lasers, Anal. Sci. 22 (2006) 1483-1487.

[10] A. Li, T. Uchimura, Y. Watanabe-Ezoe, T. Imasaka, Analysis of dioxins by gas chromatography/resonance-enhanced multiphoton ionization/mass spectrometry using nanosecond and picosecond lasers, Anal. Chem. 83 (2011) 60-66.

[11] N. Nakamura, T. Uchimura, Y. Watanabe-Ezoe, T. Imasaka, Polychlorinated aromatic hydrocarbons in a soil sample measured using gas chromatography/multiphoton ionization/time-of-flight mass spectrometry, Anal. Sci. 27 (2011) 617-622.

[12] M. Matsumoto, C.H. Lin, T. Imasaka, Enhancement of molecular ion peak from halogenated benzenes and phenols using femtosecond laser pulses in supersonic beam/time-of-flight mass spectrometry, Anal. Chem. 69 (1997) 4524-4529.

[13] J. Matsumoto, T. Imasaka, Effect of laser pulsewidth on ionization efficiency in supersonic beam-multiphoton ionization-mass spectrometry, Anal. Chem. 71 (1999) 3763-3768.

[14] A. Li, T. Imasaka, T. Imasaka, Optimal laser wavelength for femtosecond ionization of polycyclic aromatic hydrocarbons and their nitrated compounds in mass spectrometry, Anal. Chem. 90 (2018) 2963-2969.
[15] H. Kouno, T. Imasaka, The efficiencies of resonant and nonresonant multiphoton ionization in the femtosecond region, Analyst 141 (2016) 5274-5280.
[16] J. Tiantian, K. Yoshinaga, T. Imasaka, H. Nakamura, T. Imasaka, Time-correlated single ion counting mass spectrometer with long and short time-of-flight tubes and an evaluation of its performance for use in trace analysis of allergenic substances, Anal. Sci. 36 (2020) 539-543.
[17] J. Matsumoto, B. Nakano, T. Imasaka, Development of a compact supersonic jet/multiphoton ionization/time-of-flight mass spectrometer for the on-site analysis of dioxin, Part I, Evaluation of basic performance, Anal. Sci. 19 (2003) 379-382.
[18] J. Matsumoto, B. Nakano, T. Imasaka, Development of a compact supersonic jet/multiphoton ionization/time-of-flight mass spectrometer for the on-site analysis of dioxin, Part II, Application to chlorobenzene and dibenzofuran, Anal. Sci. 19 (2003) 383-386.
[19] T. Onoda, G. Saito, T. Imasaka, Scheme for collinear ionization in supersonic jet/multiphoton ionization/time-of-flight mass spectrometry, Anal. Chim. Acta 412 (2000) 213-219.
[20] T. Uchimura, S. Yamaguchi, T. Imasaka, Development of an off-axis sample introduction system for use in multiphoton ionization/time-of-flight mass spectrometry, Chem. Lett. 38 (2009) 744-745.
[21] S. Yamaguchi, F. Kira, Y. Miyoshi, T. Uchimura, Y. Watanabe-Ezoe, S. Zaitsu, T. Imasaka, T. Imasaka, Near-ultraviolet femtosecond laser ionization of dioxins in gas chromatography/time-of-flight mass spectrometry, Anal. Chim. Acta 632 (2009) 229-233.
[22] T. Matsui, T. Imasaka, Signal enhancement by crossing the sample flow at a small-angle against the laser beam in multiphoton ionization mass spectrometry, Anal. Sci. 30 (2014) 445-449.
[23] S.L. Madunil, T. Imasaka, T. Imasaka, Resonant and non-resonant femtosecond ionization mass spectrometry of organochlorine pesticides, Analyst 145 (2020) 777-783.
[24] Y. Nakano, T. Imasaka, T. Imasaka, Generation of a nearly-monocycle optical pulse in the near-infrared region and its use as an ionization source in mass spectrometry, Anal. Chem. 92 (2020) 7130-7138.
[25] T.D. Phan, A. Li, H. Nakamura, T. Imasaka, T. Imasaka, Single-photon ionization mass spectrometry using a vacuum ultraviolet femtosecond laser, J. Am. Soc. Mass Spectrom. 31 (2020) 1730-1737.
[26] S. Shibuta, T. Imasaka, T. Imasaka, Determination of fragrance allergens by ultraviolet femtosecond laser ionization mass spectrometry, Anal. Chem. 88 (2016) 10693-10700.
[27] A. Li, P.D. Thang, T. Imasaka, T. Imasaka, Suppression of fragmentation in multiphoton ionization mass spectrometry using a near-infrared femtosecond laser as an ionization source, Analyst 142 (2017) 3942-3947.
[28] T. Matsui, K. Fukazawa, M. Fujimoto, T. Imasaka, Analysis of persistent organic pollutants at sub-

femtogram levels using a high-power picosecond laser in gas chromatography/multiphoton ionization/time-of-flight mass spectrometry, Anal. Sci. 28 (2012) 445-450.
[29] A. Li, T. Uchimura, Y. Watanabe-Ezoe, T. Imasaka, Analysis of dioxins by gas chromatography/resonance-enhanced multiphoton ionization/mass spectrometry using nanosecond and picosecond lasers, Anal. Chem. 83 (2011) 60-66.
[30] T. Matsui, T. Uchimura, T. Imasaka, Gas chromatography/multiphoton ionization/time-of-flight mass spectrometry of polychlorinated biphenyls, Anal. Chim. Acta 694 (2011) 108-114.
[31] A. Li, T. Imasaka, Internal standards for use in the comprehensive analysis of polychlorinated aromatic hydrocarbons using gas chromatography combined with multiphoton ionization mass spectrometry, J. Chromatogr. A 1470 (2016) 111-117.
[32] T. Imasaka, N. Nakamura, Y. Sakoda, S. Yamaguchi, Y. Watanabe-Ezoe, T. Uchimura, T. Imasaka, Data processing technique in gas chromatography/time-of-flight mass spectrometry, Analyst 134 (2009) 712-718.
[33] Y. Watanabe-Ezoe, X. Li, T. Imasaka, T. Uchimura, T. Imasaka, Gas chromatography/femtosecond multiphoton ionization/time-of-flight mass spectrometry of dioxins, Anal. Chem. 82 (2010) 6519-6525.
[34] Y.C. Chang, T. Imasaka, Simple pretreatment procedure combined with gas chromatography/multiphoton ionization/mass spectrometry for the analysis of dioxins in soil samples obtained after the Tōhoku Earthquake, Anal. Chem. 85 (2013) 349-354.
[35] V.T.T. Duong, V. Duong, N.T.H. Lien, T. Imasaka, Y. Tang, S. Shibuta, A. Hamachi, D.Q. Hoa, T. Imasaka, Detection of polychlorinated biphenyls in transformer oils in Vietnam by multiphoton ionization mass spectrometry using a far-ultraviolet femtosecond laser as an ionization source, Talanta, 149 (2016) 275-279.
[36] O. Shitamichi, T. Imasaka, T. Uchimura, T. Imasaka, Multiphoton ionization/mass spectrometry of polybrominated diphenyl ethers, Anal. Method 3 (2011) 2322-2327.
[37] N. Itouyama, T. Matsui, S. Yamamoto, T. Imasaka, T. imasaka, Analysis of parent/nitrated polycyclic aromatic hydrocarbons in particulate matter 2.5 based on gas chromatography/time-of-flight mass spectrometry using a femtosecond laser as the ionization source, J. Amer. Soc. Mass Spectrom. 27 (2016) 293-300.
[38] Y. Tang, T. Imasaka, S. Yamamoto, T. Imasaka, Multiphoton ionization mass spectrometry of nitrated polycyclic aromatic hydrocarbons, Talanta 140 (2015) 109-114.
[39] Y. Tang, T. Imasaka, S. Yamamoto, T. Imasaka, Determination of polycyclic aromatic hydrocarbons and their nitro-, amino-derivatives adsorbed on particulate matter 2.5 by multiphoton ionization mass spectrometry using far-, deep-, and near-ultraviolet femtosecond lasers, Chemosphere 152 (2016) 252-258.
[40] A. Li, T. Imasaka, T. Uchimura, T. Imasaka, Analysis of pesticides by gas chromatography/multiphoton

ionization/mass spectrometry using a femtosecond laser, Anal. Chim. Acta 701 (2011) 52-59.
[41] X. Yang, T. Imasaka, T. Imasaka, Determination of pesticides by gas chromatography combined with mass spectrometry using femtosecond lasers emitting at 267, 400, and 800 nm as the ionization source, Anal. Chem. 90 (2018) 4886-4893.
[42] Y. Hashiguchi, S. Zaitsu, T. Imasaka, Ionization of pesticides using a far-ultraviolet femtosecond laser in gas chromatography/time-of-flight mass spectrometry, Anal. Bioanal. Chem. 405 (2013) 7053-7059.
[43] X. Yang, T. Imasaka, A. Li, T. Imasaka, Determination of hexachlorocyclohexane by gas chromatography combined with femtosecond laser ionization mass spectrometry, J. Amer. Soc. Mass Spectrom. 27 (2016) 1999-2005.
[44] S. Yamaguchi, T. Uchimura, T. Imasaka, T. Imasaka, Gas chromatography/time-of-flight mass spectrometry of triacetone triperoxide based on femtosecond laser ionization, Rapid Commun. Mass Spectrom. 23 (2009) 3101-3106.
[45] T. Shimizu, Y. Watanabe-Ezoe, S. Yamaguchi, H. Tsukatani, T. Imasaka, S. Zaitsu, T. Uchimura, T. Imasaka, Enhancement of molecular ions in mass spectrometry using an ultrashort optical pulse in multiphoton ionization, Anal. Chem. 82 (2010) 3441-3444.
[46] A. Hamachi, T. Okuno, T. Imasaka, Y. Kida, T. Imasaka, Resonant and nonresonant multiphoton ionization processes in the mass spectrometry of explosives, Anal. Chem. 87 (2015) 3027-3031.
[47] R. Ezoe, T. Imasaka, T. Imasaka, Determination of triacetone triperoxide using ultraviolet femtosecond multiphoton ionization time-of-flight mass spectrometry, Anal. Chim. Acta 853 (2015) 508-513.
[48] T. Fujii, T. Imasaka, T. Imasaka, Use of chemical conversion for determination of nitrated aromatic hydrocarbons using femtosecond ionization mass spectrometry, Anal. Chim. Acta 996 (2017) 48-53.
[49] Y. Tang, S. Yamamoto, A. Li, T. Imasaka, Determination of nitrated polycyclic aromatic hydrocarbons in particulate matter 2.5 by laser ionization mass spectrometry using an on-line chemical-reduction system, Analyst 144 (2019) 2909-2913.
[50] A. Hamachi, T. Imasaka, H. Nakamura, A. Li, T. Imasaka, Determination of nerve agent metabolites by ultraviolet femtosecond laser ionization mass spectrometry, Anal. Chem. 89 (2017) 5030−5035.
[51] V.V. Son, H. Nakamura, T. Imasaka, T. Imasaka, Determination of nerve agent metabolites in human urine by femtosecond laser ionization mass spectrometry using 2-(bromomethyl)naphthalene as a derivatizing reagent, Anal. Chim. Acta 1069 (2019) 82-88.

Figure Captions

Fig. 1. Schematic picture showing a mass spectrum of an organic compound.

Fig. 2. Energy diagrams (A) RE2PI and NRMPI using UV and NIR lasers, respectively (B) RE2PI and NR2PI using a UV laser. When the excitation energy (*EE*) is larger than half of the ionization energy (*IE*), RE2PI provides a large excess energy that results in the dissociation of a molecular ion. On the other hand, NR2PI provides a lower ionization efficiency but

excess energy is minimized and suppresses fragmentation.

Fig. 3. Schematic of the experimental apparatus used for GC-MS.

Fig. 4. Ionization schemes: (A) conventional (B) proximity configurations. (C) structure of the nozzle, consisting of an assembly composed of a ring-repeller and double-skimmer-type extraction/ground electrodes for ion acceleration. The ion beam is focused by an einzel lens electrode assembly and is focused onto a microchannel plate detector (not shown) using two couples of deflector electrodes.

Fig. 5. Photograph of the optical system used for the generation and measurement of an ultrashort optical pulse.

Fig. 6. Schematic of the experimental apparatus used to generate an VUV pulse. M, mirror; λ/2, half wave plate; BBO, β-barium borate crystal; TP, time plate; DM, dichroic mirror; CM, concave mirror; CaF_2, calcium fluoride window (reproduced from ref. [24], with permission from American Chemical Society).

Fig. 7. Spectrogram of a Raman emission. The visible part is attenuated to enhance the UV part. The NIR beams (>800 nm) are not observed in the picture due to the limited sensitivity of the charge-coupled-device (CCD) camera (reproduced from ref. [24], with permission from the American Chemical Society).

Fig. 8. Ionization schemes for (A) RE2PI (B) NR2PI (C) NR3PI. The rate constants are defined as follows: k_1, excitation; k_2, ionization; k_{flu}, fluorescence, k_{IC}, intersystem crossing; k_{phos}, phosphorescence; k_{12}, NR2PI; k_{123}, NR3PI; k_3, autodissociation; k_4, photodissociation. ΔE_{excess}, excess energy; M^+, molecular ion: F^+, fragment ion; F, neutral fragment; S_0, ground state; S_1, excited state (reproduced from ref. [22], with permission from the Royal Society of Chemistry).

Fig. 9. Two-dimensional display of GC-MS (A) all area of the data (B) expanded part specified by a pink square in (A) measured for a soil sample containing halogenated organic compounds. CN, chlorinated naphthalene; CB, chlorinated biphenyl; CDF, chlorinated dibenzofuran; CDD, chlorinated dibenzo-*p*-dioxin, CT, chlorinated terphenyl, PeCDF, pentachlorodibenzofuran. *m/z*, mass-to-charge ratio (reproduced from ref. [31], with permission from the Royal Society of Chemistry).

Fig. 10. Two-dimensional display of GC-MS for a sample containing (A) no polychlorinated CB/DF/DD/T (B) tetra- (Te), penta- (Pe), hexa- (Hx), hepta- (Hp), octa- (Oc), and nona- (Nona)CBs (reproduced from ref. [33], with permission from the American Chemical Society).

Fig. 11. Mass spectra measured for (A) 9-NAT (B) 3-NFLU (C) 1-NPYR. M^+, molecular ion; (1) – (4), fragment ions. The wavelength of the laser used for ionization is shown in the figure (reproduced from ref. [37], with permission from Elsevier).

Fig. 12. Schematic energy diagram and ionization scheme for (A) 9-NAT (B) 3-NFLU (C) 1-NPYR. The wavelength of the laser used for ionization is shown by red color (reproduced from ref. [37], with permission from Elsevier).

Fig. 13. Two-dimensional display of GC-MS measured for a sample extracted from PM2.5 at (A) 200 (B) 267 (C) 345 nm (reproduced from ref. [38], with permission from Elsevier).

Fig. 14. Chemical structures of allergenic compounds specified in the Cosmetics Directive published by the Scientific Committee for Consumer Safety. The chemical structure comprising an aliphatic long chain is specified by blue color (reproduced from ref. [26], with permission from the American Chemical Society).

Fig. 15. Two-dimensional display of GC-MS measured for a real sample (A) Sakura Eau de Toilette (B) Moroccan Rose. The assigned constituents are shown in the figure (reproduced from ref. [26], with permission from the American Chemical Society).

Fig. 16. Chemical structure of pesticides in a standard sample mixture. A variety of compounds with different chemical structures are contained in the sample (reproduced from ref. [40], with permission from the American Chemical Society).

Fig. 17. (A) chemical structure of TATP. The mass spectrum is measured at (B) 219 nm (C) 241 nm (D) 267 nm. A molecular ion, $[M]^+$, is strongly enhanced at 267 nm, suggesting minimal excess energy at this wavelength (reproduced from ref. [49], with permission from the American Chemical Society).

Fig. 18. Two-dimensional display of GC-MS measured for a sample of human blood containing TATP (A) without and (B) with acetone measured at three days after the sample preparation. TATP-d18 synthesized using deuterated acetone was added in the sample for use as an internal standard (reproduced from ref. [46], with permission from Elsevier).

Fig. 19. Two-dimensional displays of GC-MS for a sample extracted from PM2.5 measured (A) (C) without and (B) (D) with a reducing reagent of hydrazine monohydrate (reproduced from ref. [47], with permission from Elsevier).

Fig. 20. Derivatization of nerve agent metabolites (e.g., IMPA) using 2-(bromomethyl)naphthalene (BMN).

Fig. 21. Two-dimensional display of GC-MS measured for a sample containing EMPA, IMPA, and PMPA in human urine. The analytes were extracted from urine with diethyl ether and were

derivatized with BMN. Two isomers were observed for PMPA. Yellow solid circle; BMN and the side-reaction products; yellow broken line, fragments of MN-EMPA, MN-IMPA, and MN-PMPA (reproduced from ref. [50], with permission from Elsevier).

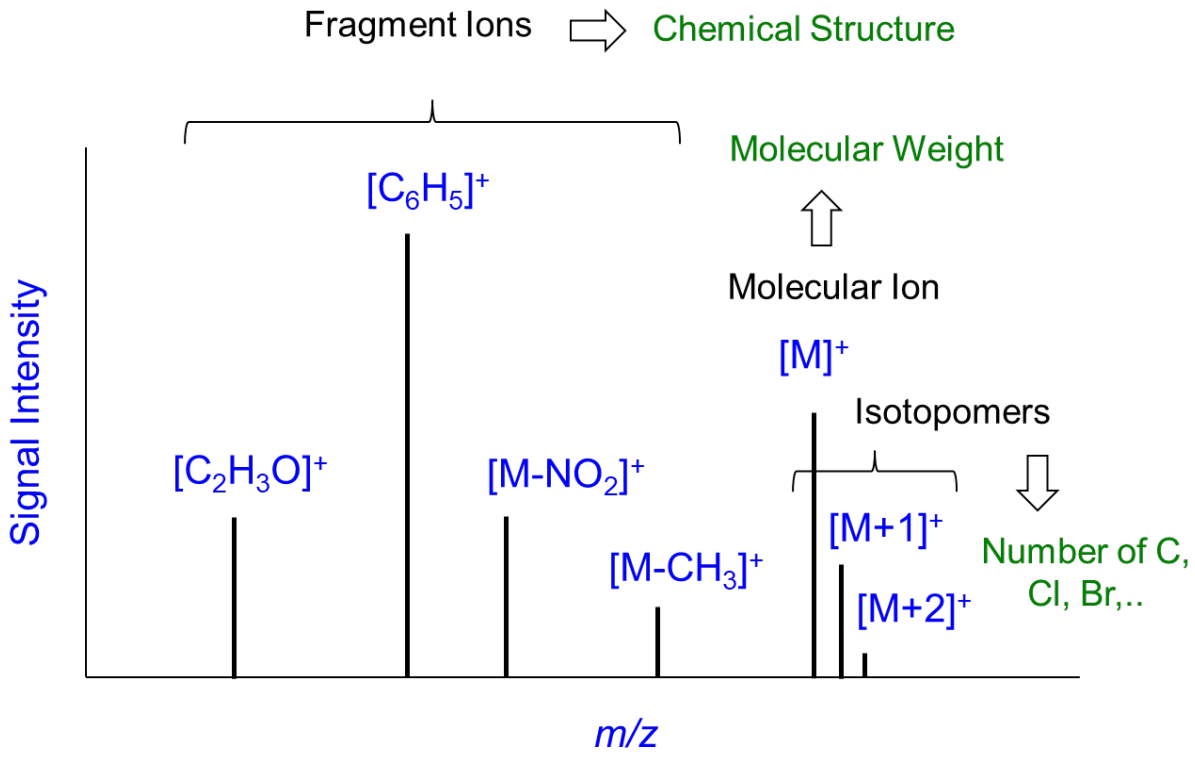

Fig. 1 T. Imasaka and T. Imasaka

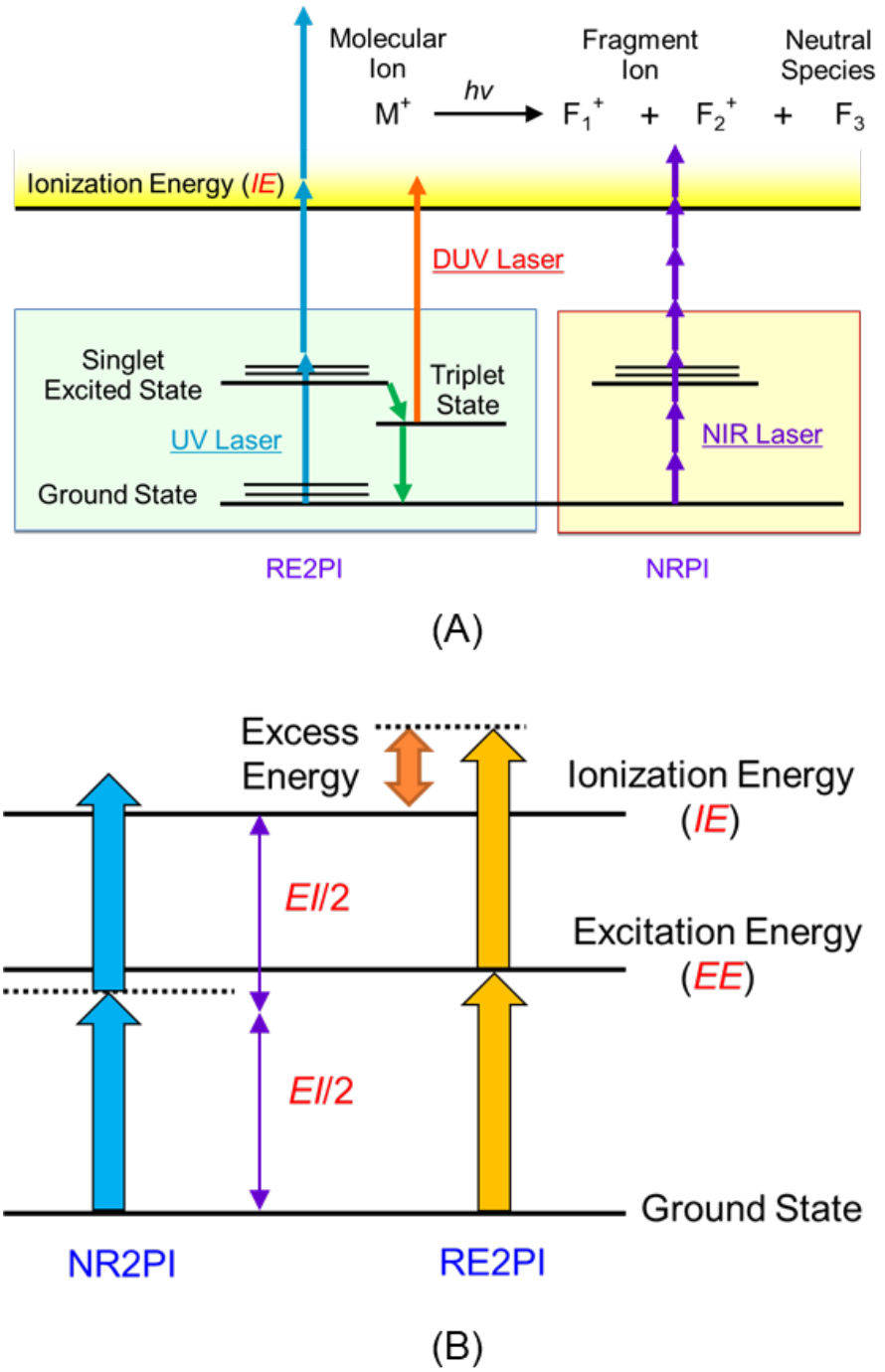

Fig. 2 T. Imasaka and T. Imasaka

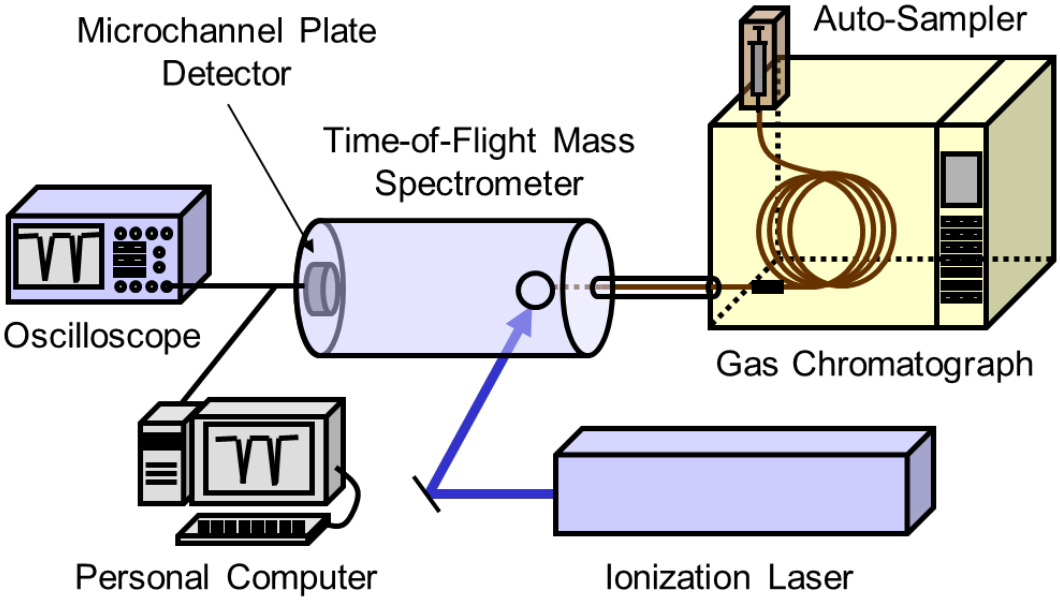

Fig. 3 T. Imasaka and T. Imasaka

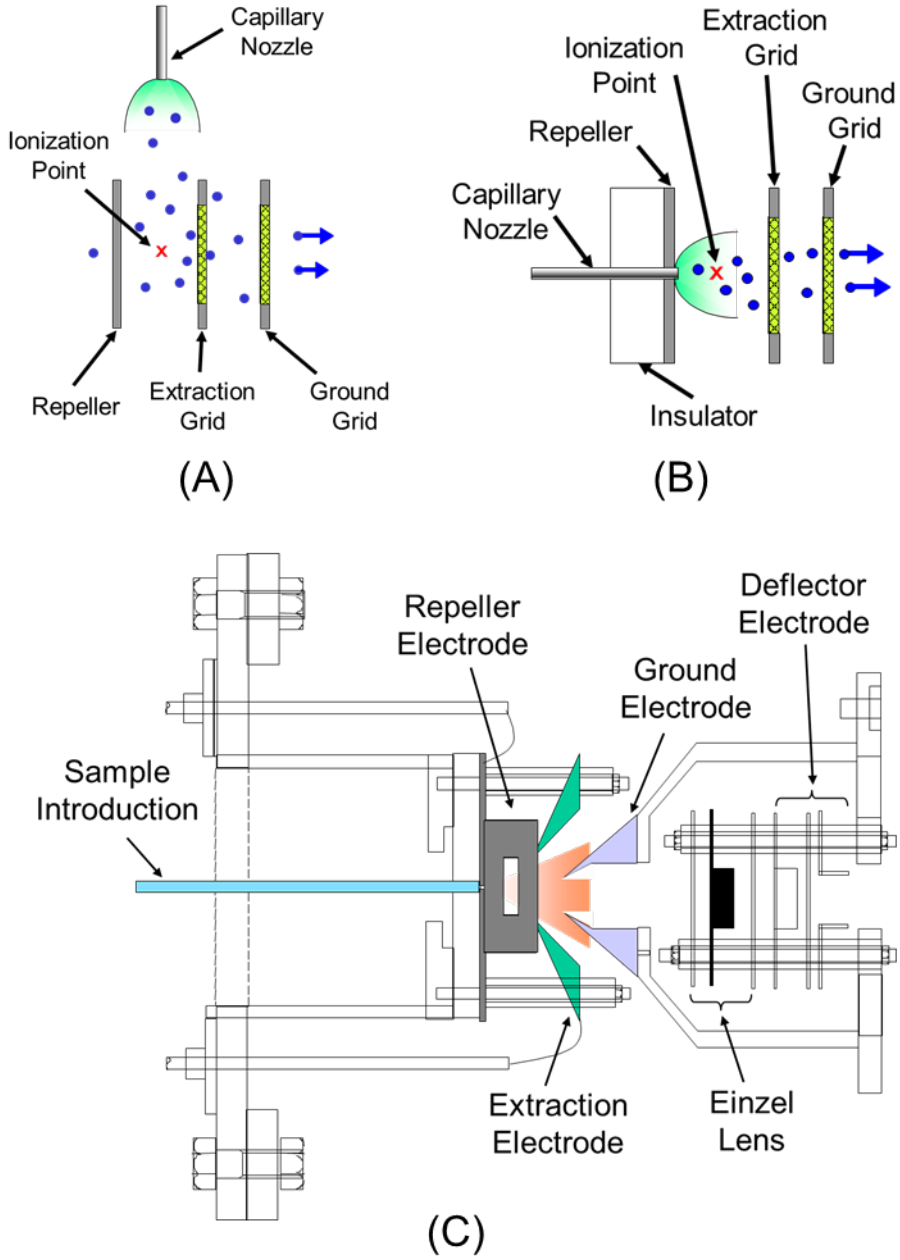

Fig. 4 T. Imasaka and T. Imasaka

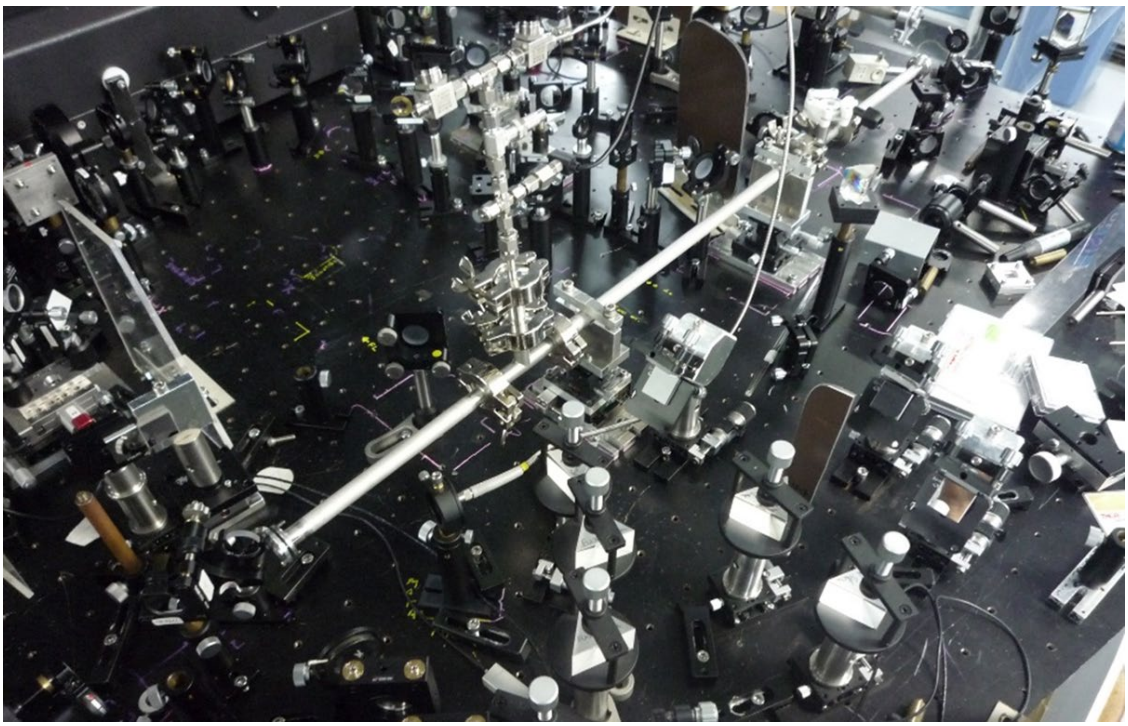

Fig. 5 T. Imasaka and T. Imasaka

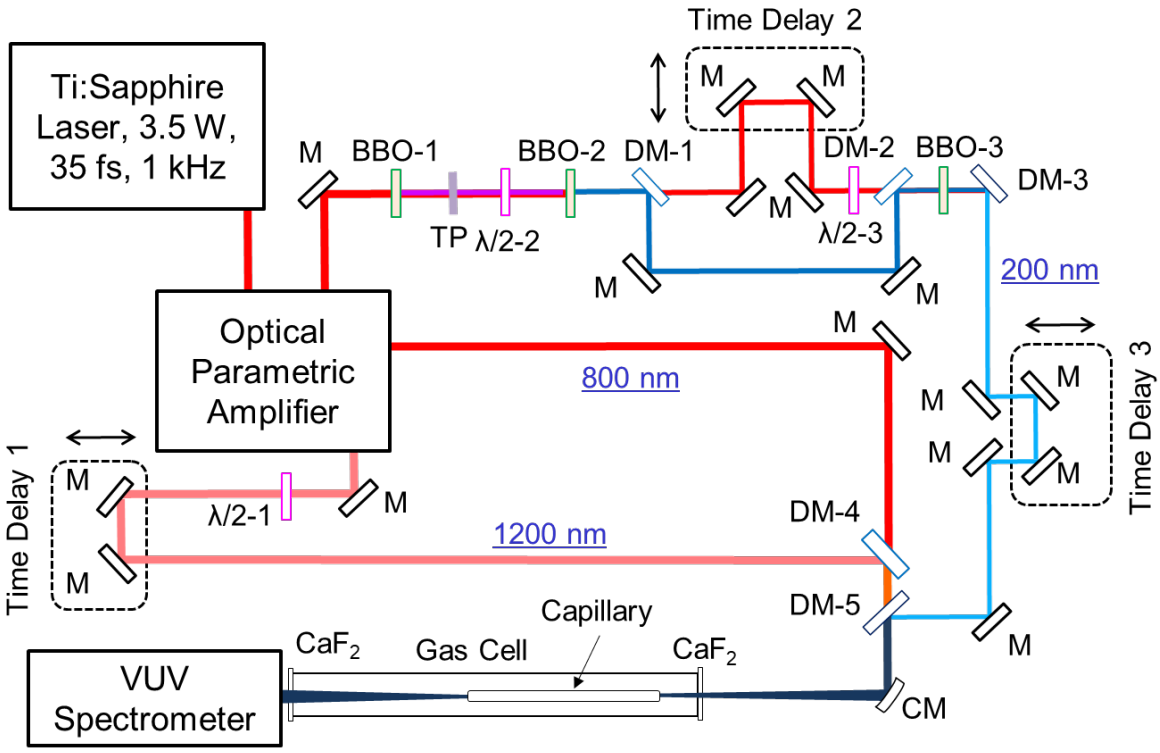

Fig. 6 T. Imasaka and T. Imasaka

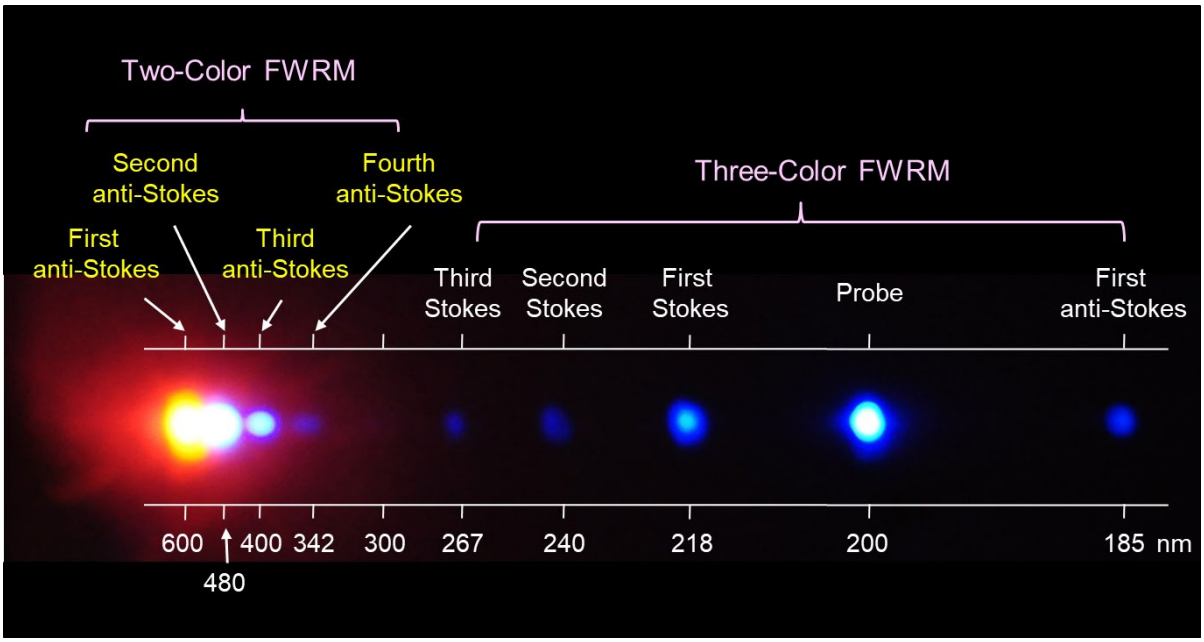

Fig. 7 T. Imasaka and T. Imasaka

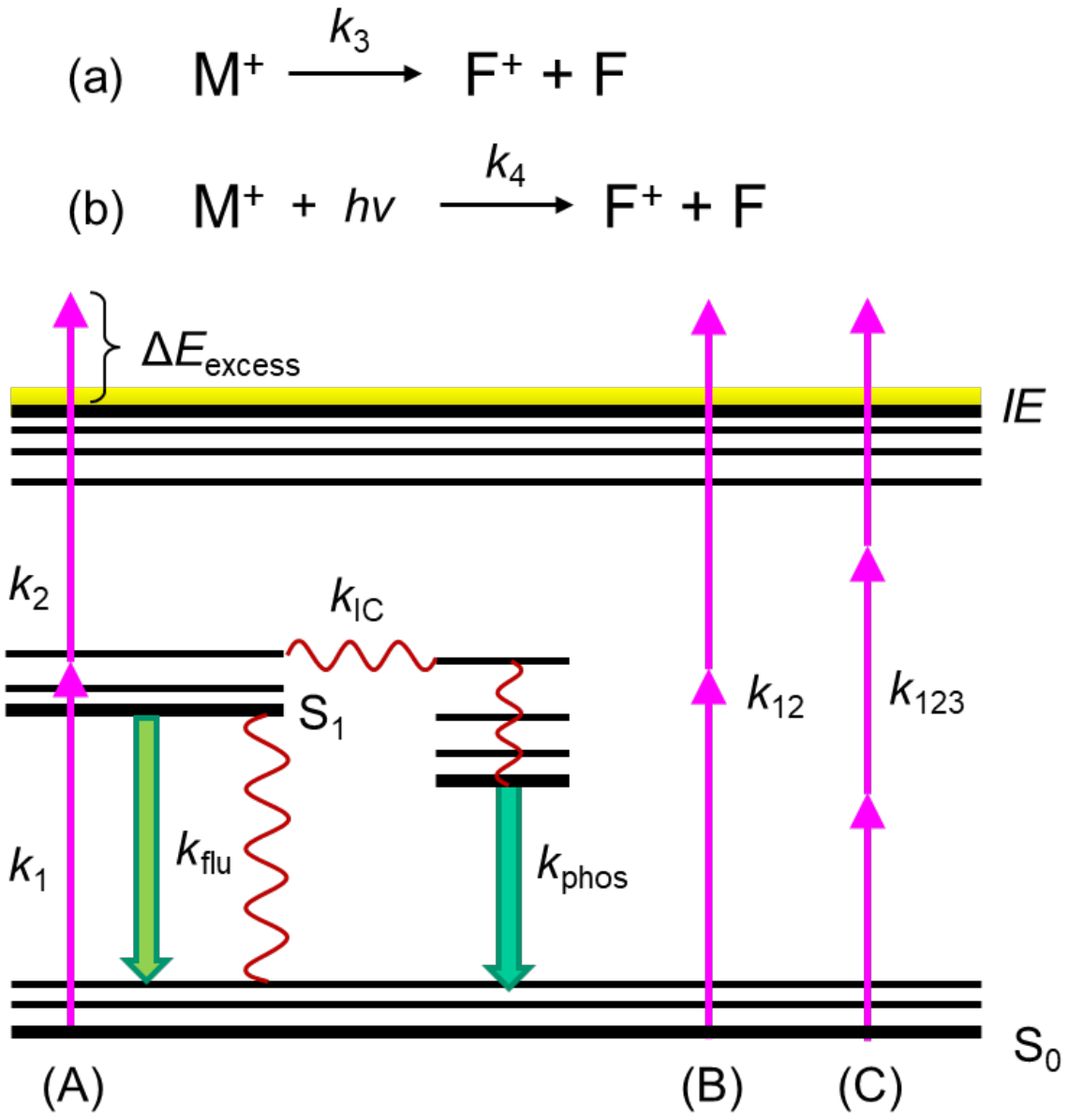

Fig. 8 T. Imasaka and T. Imasaka

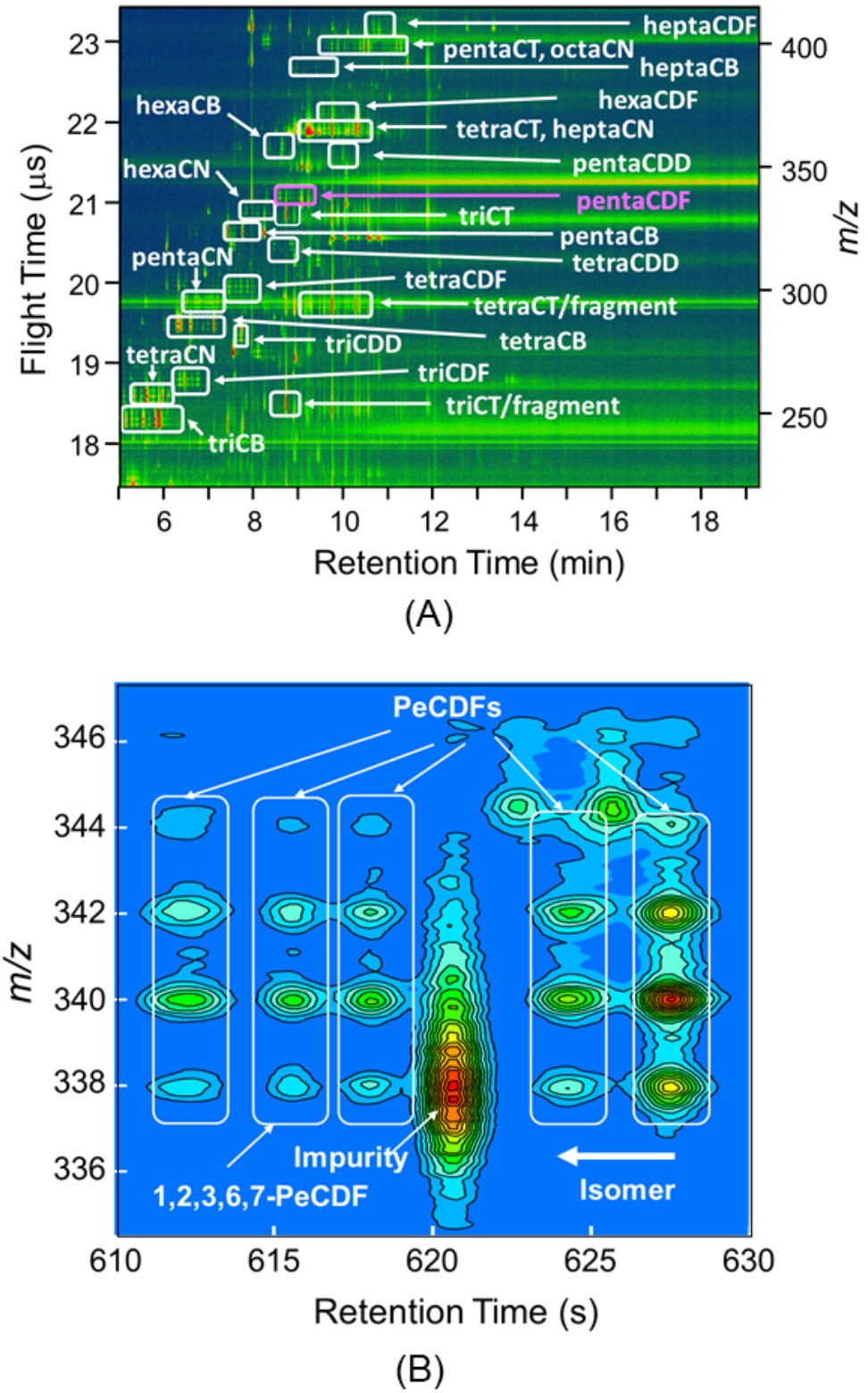

Fig. 9 T. Imasaka and T. Imasaka

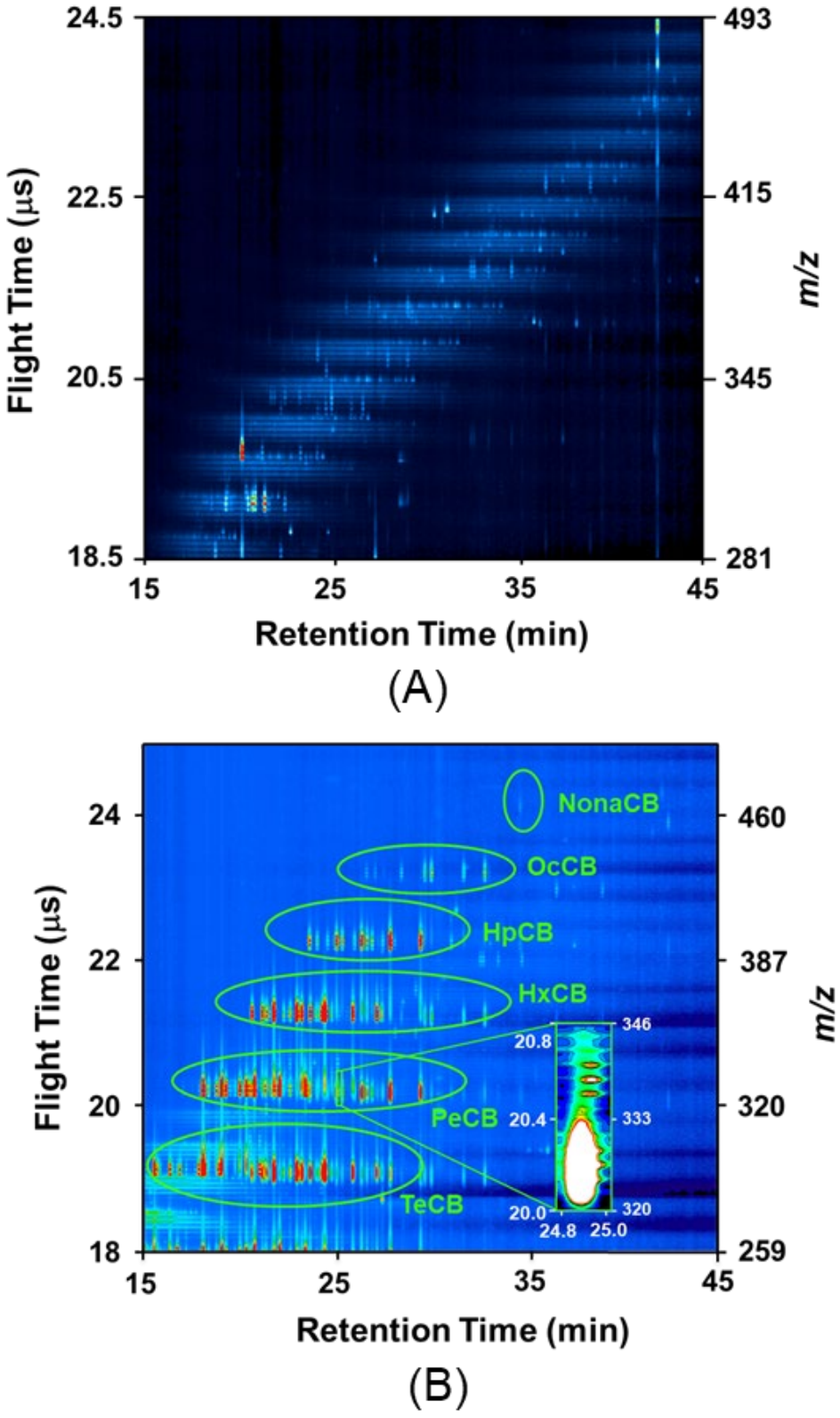

Fig. 10 T. Imasaka and T. Imasaka

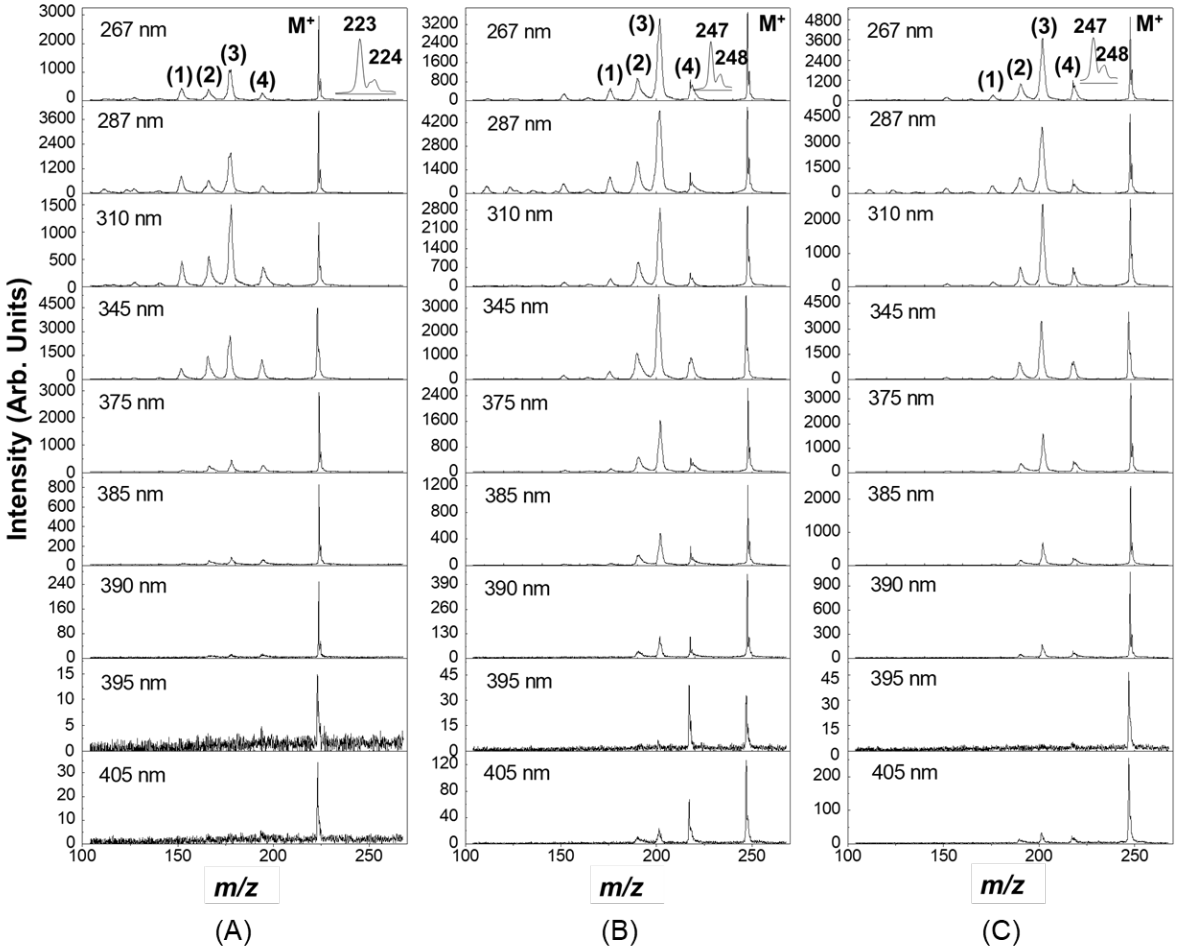

Fig. 11 T. Imasaka and T. Imasaka

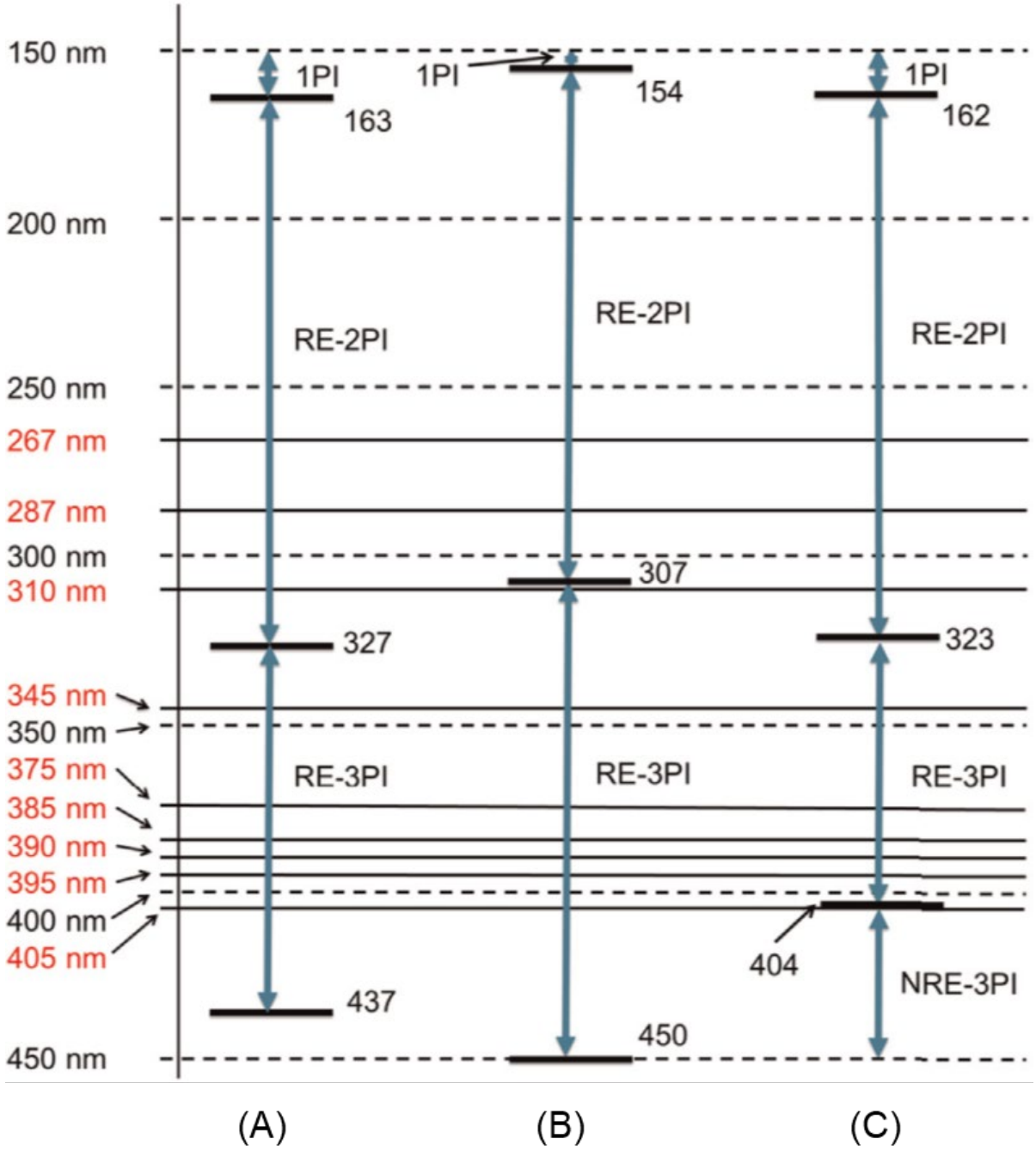

Fig. 12 T. Imasaka and T. Imasaka

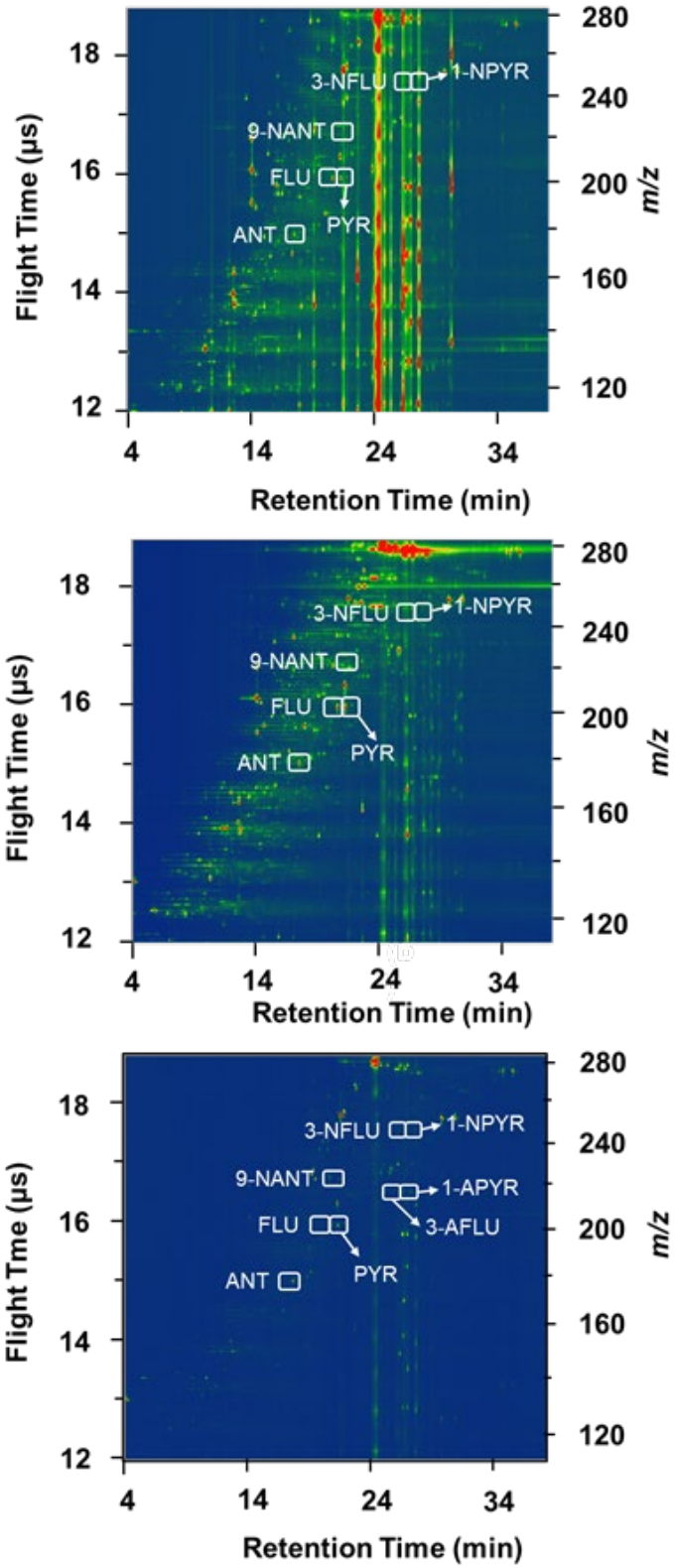

Fig. 13 T. Imasaka and T. Imasaka

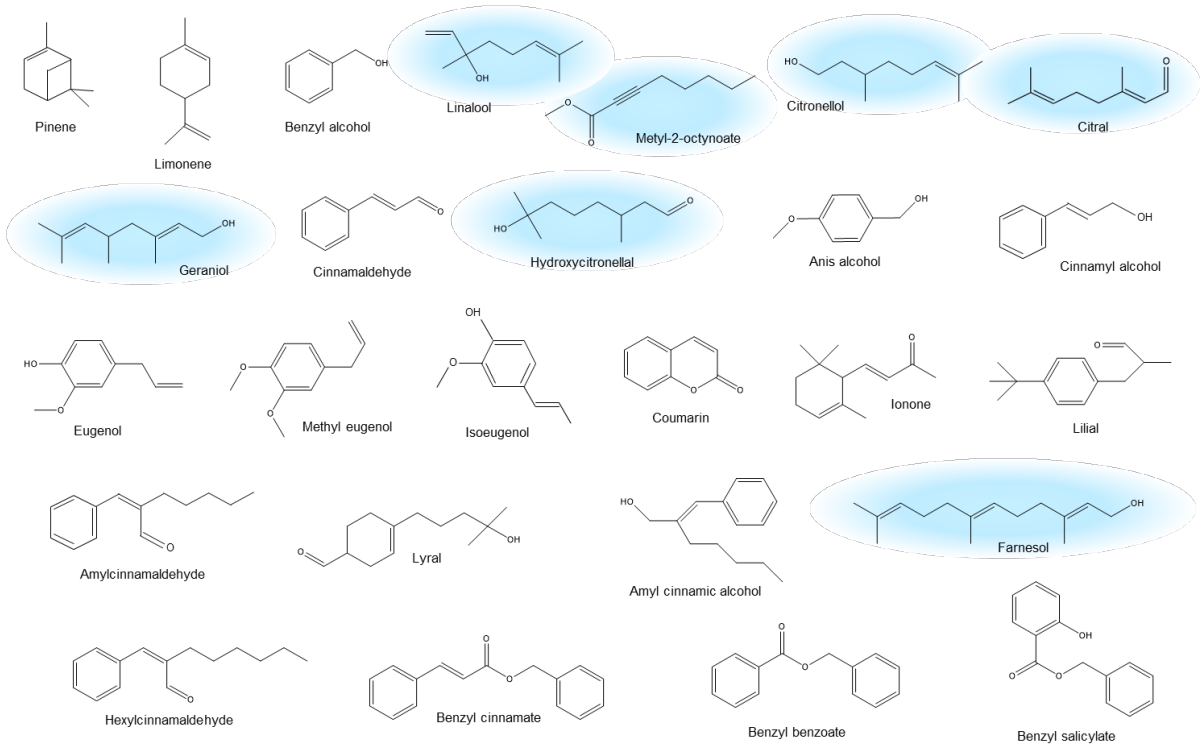

Fig. 14 T. Imasaka and T. Imasaka

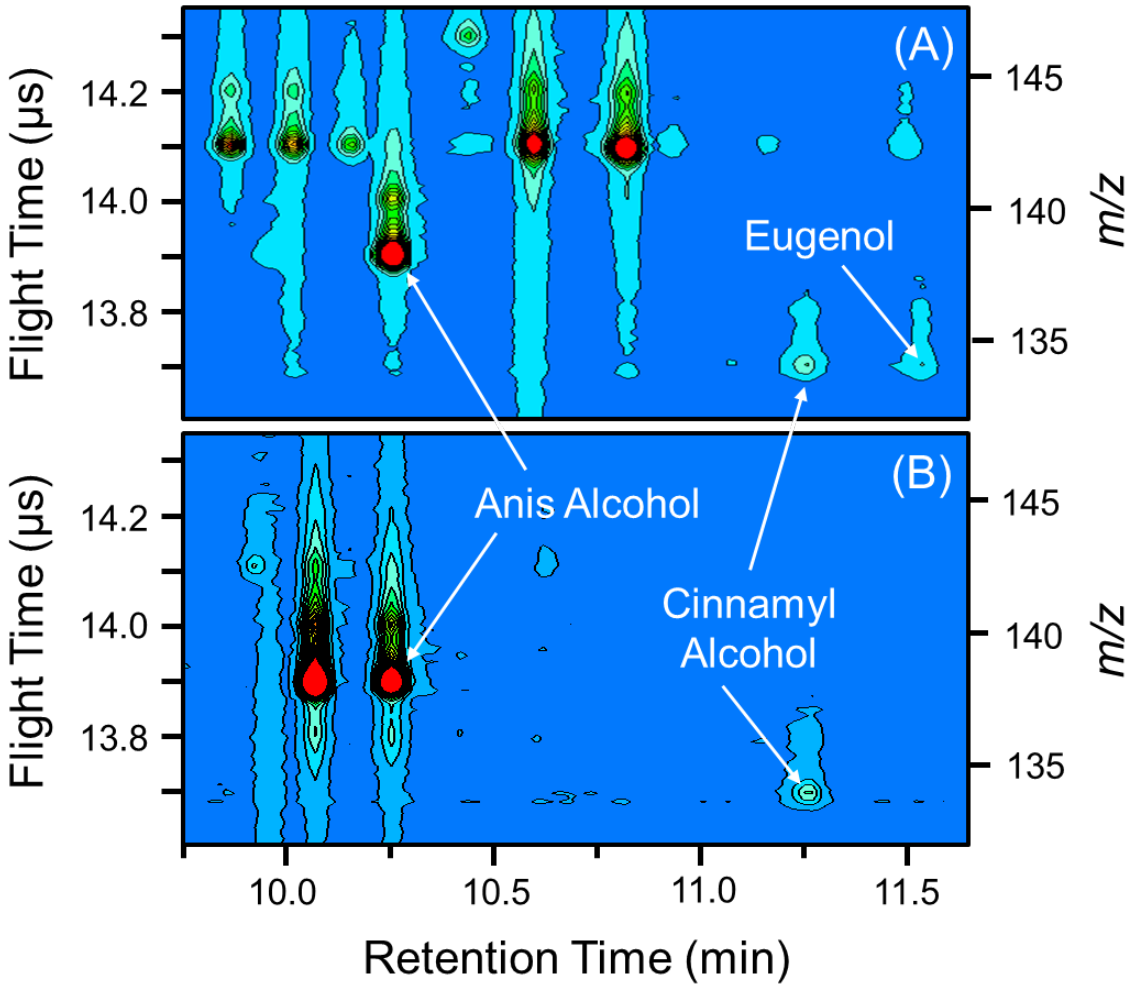

Fig. 15 T. Imasaka and T. Imasaka

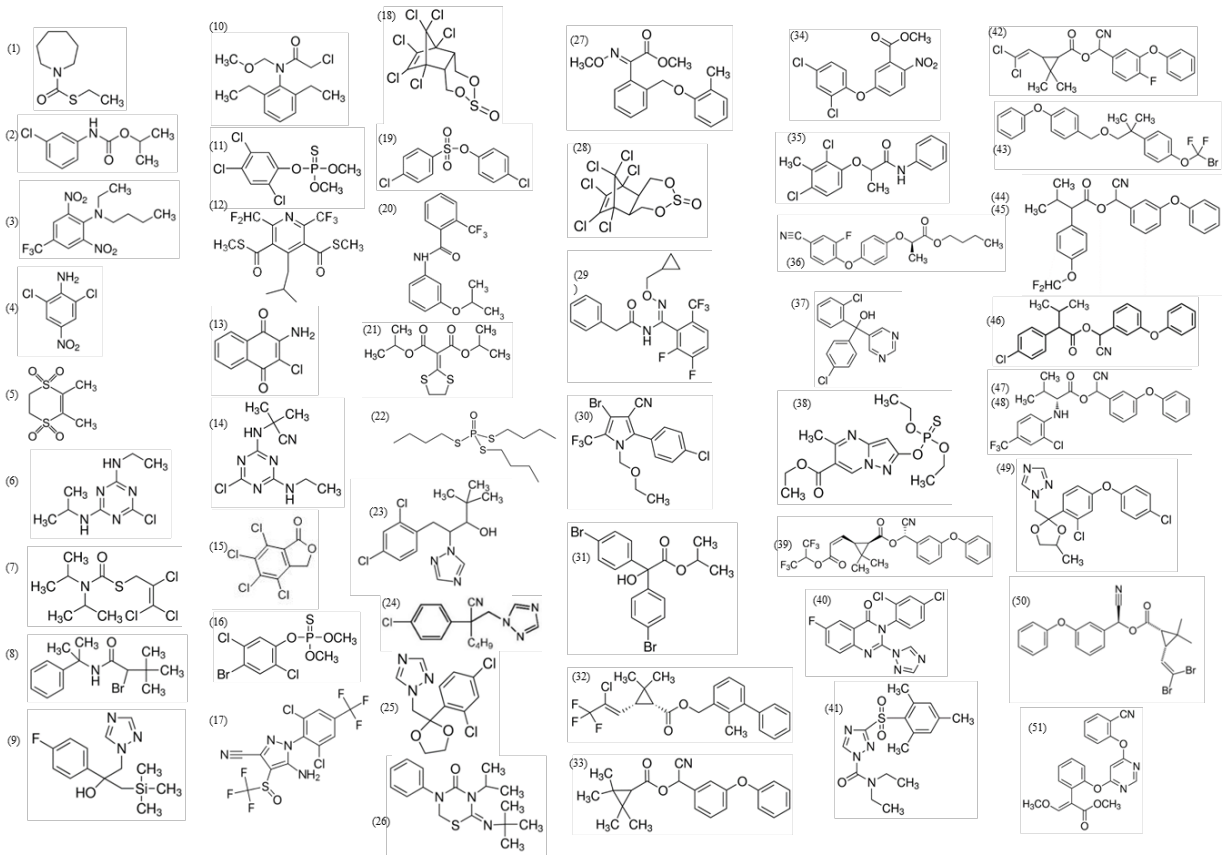

Fig. 16 T. Imasaka and T. Imasaka

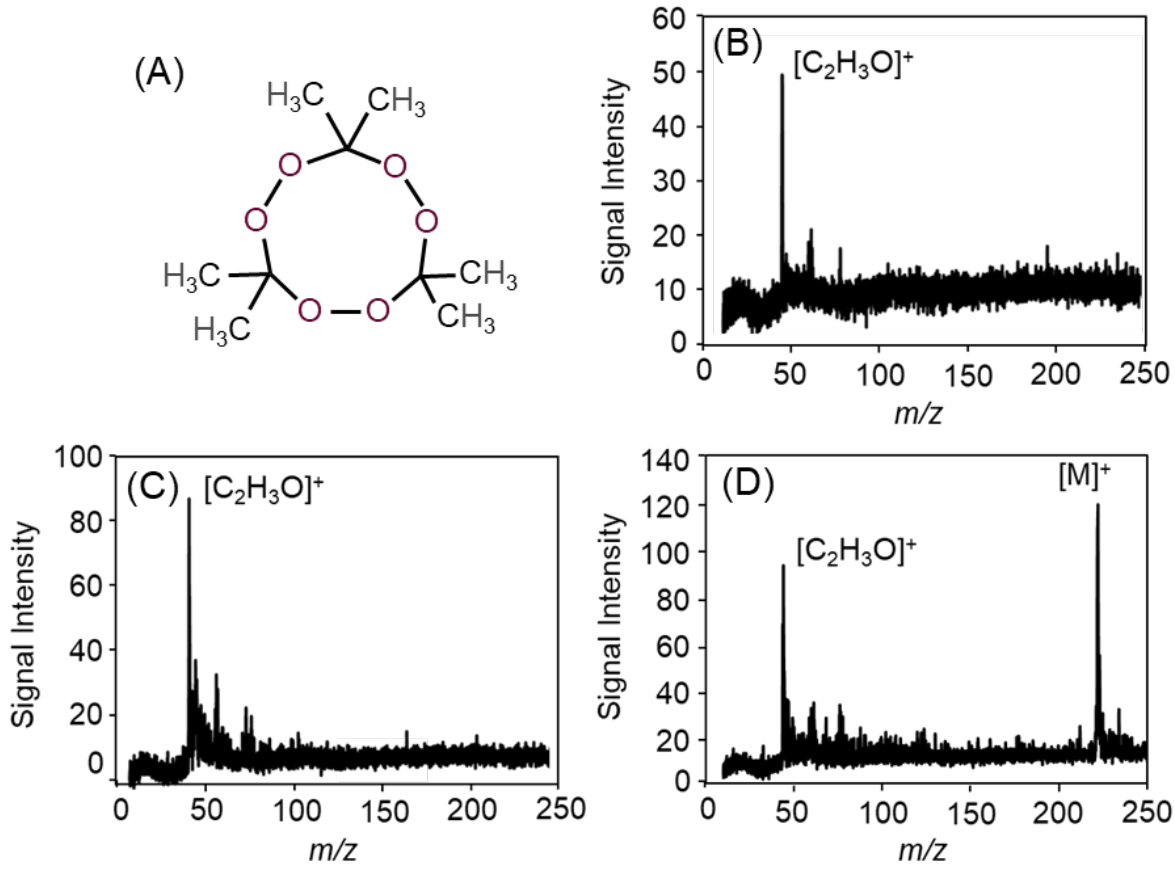

Fig. 17 T. Imasaka and T. Imasaka

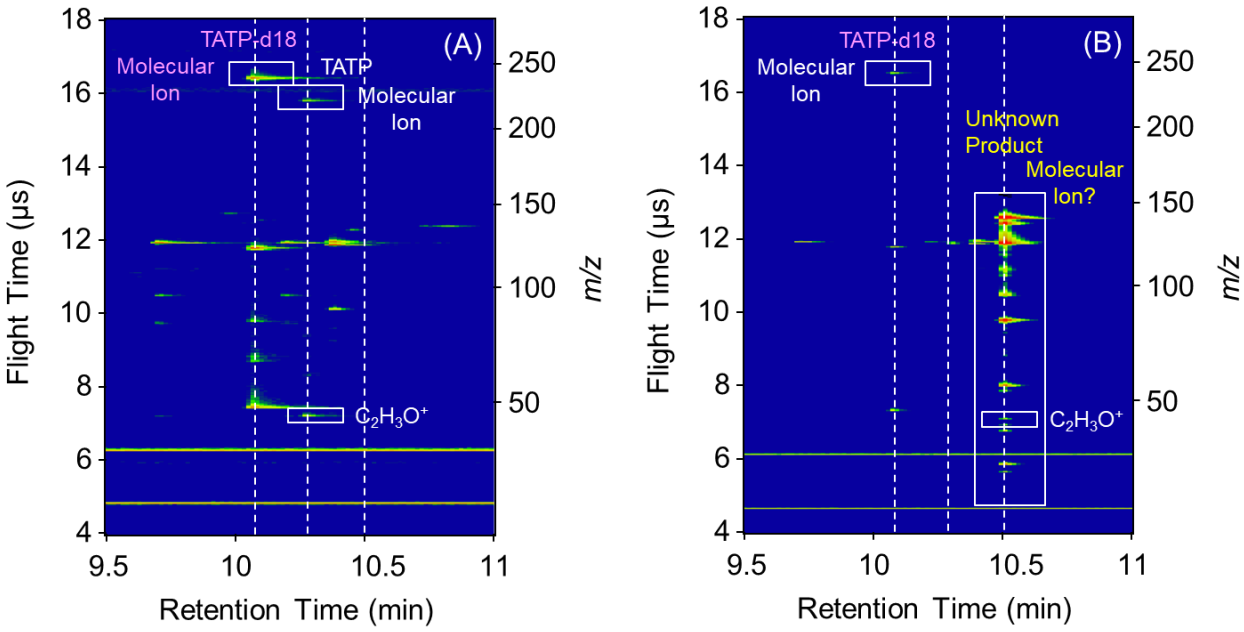

Fig. 18 T. Imasaka and T. Imasaka

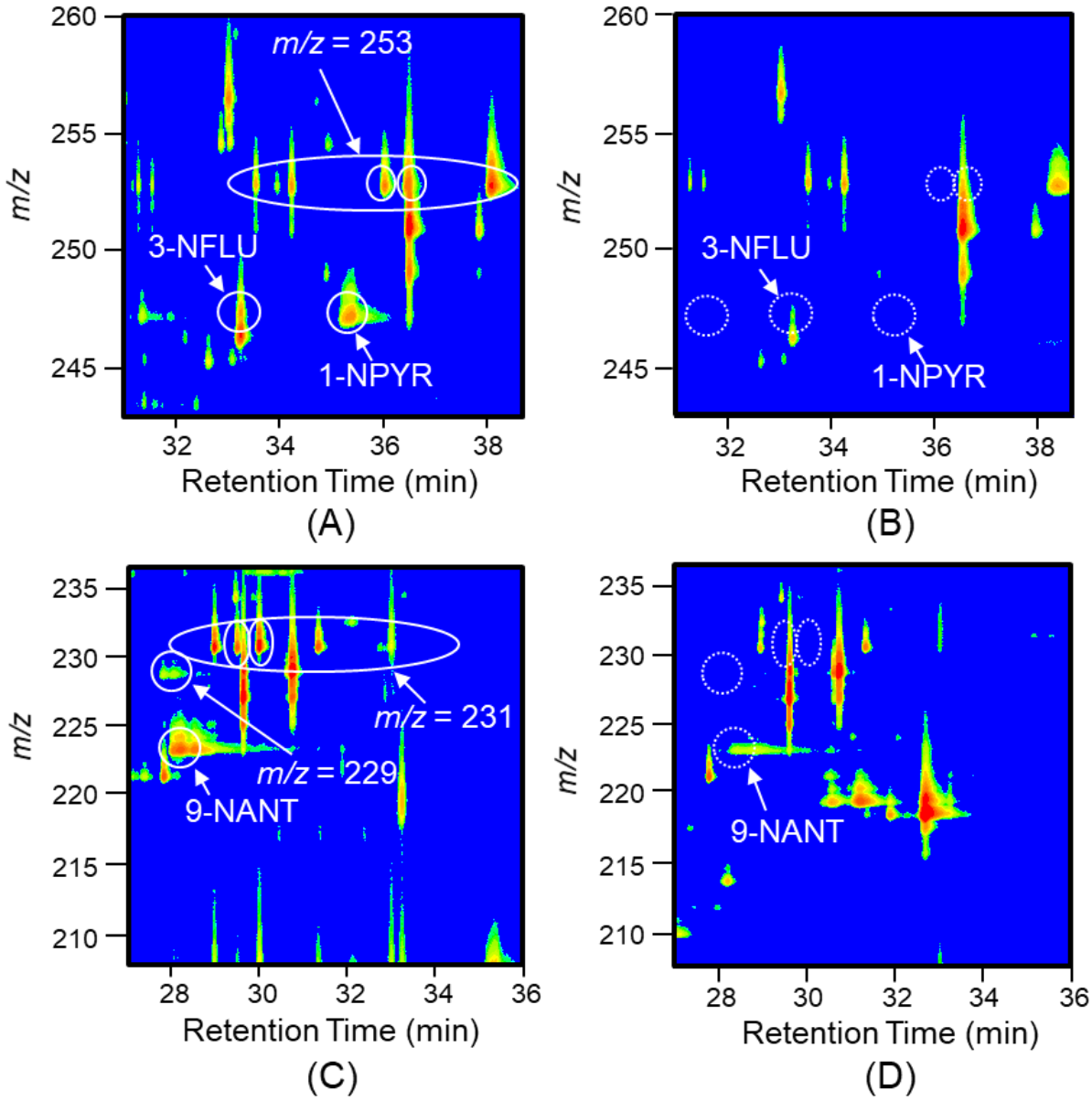

Fig. 19 T. Imasaka and T. Imasaka

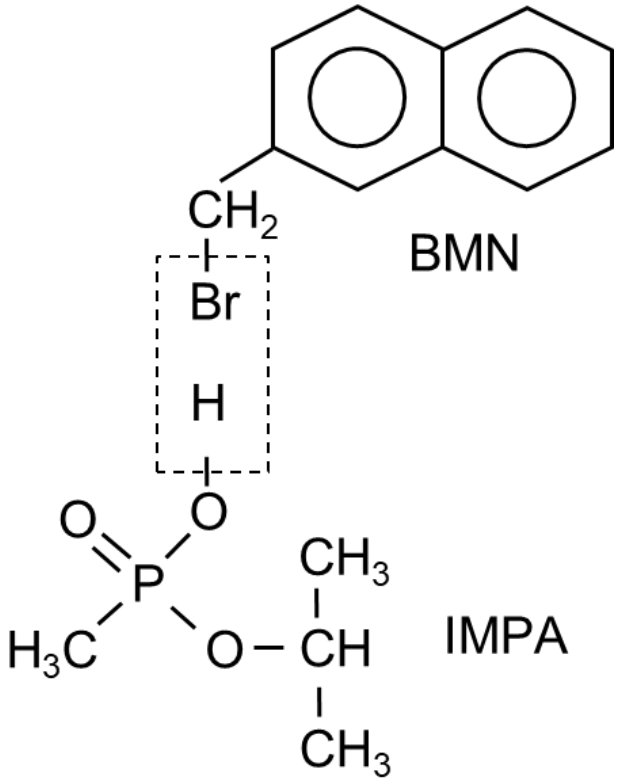

Fig. 20 T. Imasaka and T. Imasaka

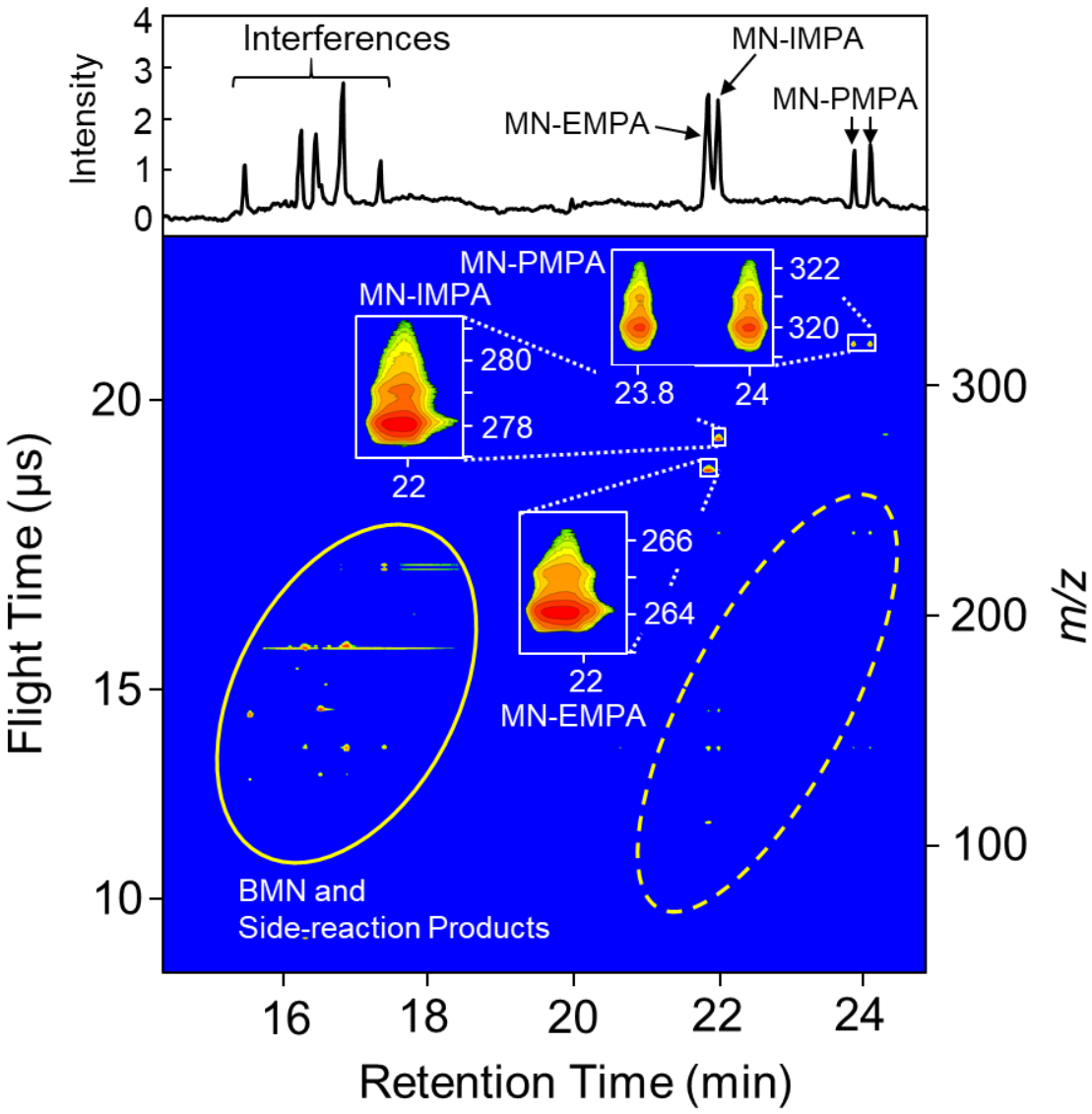

1 Fig. 21 T. Imasaka and T. Imasaka